



UNIVERSITY OF
EASTERN FINLAND

EFFECT OF ADENOVIRUSES ON LIVER XENOBIOTIC METABOLIC ENZYME ACTIVITIES IN RAT
LIVER

Jani, Väisänen

Master's thesis

Master's degree programme in General
Toxicology

University of Eastern Finland, School of
Pharmacy

May, 2022

University of Eastern Finland, Faculty of Health Sciences

School of Pharmacy

Master's Degree Programme in General Toxicology

VÄISÄNEN, JANI: Effect of adenoviruses on liver xenobiotic metabolic enzyme activities in rat liver.

Master's thesis, 50 pages, 3 appendices (5 pages)

The thesis instructors: Professor Risto Juvonen and Professor Jaana Rysä

May 2022

Keywords: adenoviruses, gene therapy, xenobiotic metabolism

Individual variance in the reaction rate of xenobiotic metabolism is high, nevertheless, the reaction rate should be in the normal range to ensure the success of drug therapy. Proper dosing is especially crucial when the drug has a narrow therapeutic range or severe adverse effects. Previous studies have shown altered metabolic activity shortly after treatment with first-generation serotype 5 adenoviruses containing the beta-galactosidase gene.

This study aimed to find out if treatment with recombinant replication-deficient adenovirus type 5 containing various transgenes causes changes in the xenobiotic metabolic activities of the Sprague-Dawley rat liver after 14 days of the treatment. Xenobiotic metabolic activity assays were carried out in liver microsomes or cytosol of treated animals *in vitro*. Reaction rates of untreated control rat liver samples (n = 4) were compared to reaction rates of rats treated with adenoviruses containing the following gene cassettes: NLS-LacZ (n = 7), LacZ (n = 6), Nkx2.5+GATA (n = 6), Nkx2.5 (n = 2), ASPEX (n = 3), PEX (n = 3), and rSMARCKD3 (n = 4).

Phase 1 cytochrome P450 (CYP) metabolic reactions were studied with substrates of CYP1 (7-ethoxyresorufin), CYP2B (7-pentoxyresorufin), and non-specific CYP substrates and 3-(3-(7-ethoxycoumarin benzyloxy)-phenyl-7-methoxycoumarin). Phase 2 conjugation reactions were studied with the substrates of UDP glucuronosyltransferase and sulfotransferase (7-hydroxy-4-trifluoromethylcoumarin), catechol-O-methyltransferase (esculetin), and glutathione S-transferase (1-chloro-2,4-dinitrobenzene).

Significant changes in reaction rate caused by adenovirus vector or transgenes were not observed in any of the samples ($p > 0.05$). Therefore, adenovirus treatment likely does not alter xenobiotic metabolic rates after 14 days of the treatment.

Itä-Suomen yliopisto, Terveystieteiden tiedekunta

Farmasian laitos

Yleisen toksikologian koulutusohjelma

VÄISÄNEN, JANI: Adenovirusten vaikutus maksan vierasainemetabolian aktiivisuuteen rotan maksassa.

Pro gradu, 50 sivua, 3 liitettä (5 sivua)

Ohjaajat: Professori Risto Juvonen ja Professori Jaana Rysä

Toukokuu 2022

Avainsanat: adenovirukset, geeniterapia, vierasainemetabolia

Yksilöllinen vaihtelu vierasainemetabolian nopeudessa on suuri. Siitä huolimatta reaktionopeuksien pitäisi pysyä normaalissa vaihteluvälissä, jotta eri lääkehoidot onnistuvat. Oikea annos on erityisen tärkeää silloin kun lääkkeellä on kapea terapeutinen leveys tai vakavia haittavaikutuksia. Aiemmassa tutkimuksessa ensimmäisen sukupolven adenovirus aiheutti metabolisen aktiivisuuden muutoksia pian viruskäsittelyn jälkeen.

Tutkimuksen tavoitteena oli tutkia, aiheuttavatko riittämättömästi replikoituvat tyypin 5 rekombinantti adenovirus tai erilaiset geenikasetit muutoksia vierasainemetabolian aktiivisuuteen Sprague-Dawley rotilla 14 päivän jälkeen. Vierasainemetabolian aktiivisuusmittaukset tehtiin maksan mikrosomi- ja sytolisnäytteistä *in vitro*. Kontrollirottien maksanäytteistä (n = 4) mitattua reaktionopeutta verrattiin käsiteltyjen rottien reaktionopeuksiin. Geenikasetit tutkimuksessa olivat: NLS-LacZ (n = 7), LacZ (n = 6), Nkx2.5+GATA (n = 6), Nkx2.5 (n = 2), ASPEX (n = 3), PEX (n = 3) ja rSMARCKD3 (n = 4).

Ensimmäisen vaiheen sytokromi P450 (CYP)-entsyymien reaktioita tutkittiin seuraavien entsyymien substraateilla: CYP1 (7-etoksiresorufiini), CYP2B (7-pentoksiresorufiini), ja ei spesifeillä CYP substraateilla (7-etoksikumariini ja 3-(3-bentsyylioksi)-fenyli-7-metoksikumariini). Toisen vaiheen konjugaatioreaktioita tutkittiin seuraavien entsyymien substraateilla: UDP-glukuronyylitransferaasi ja sulfotransferaasi (7-hydroksi-4-trifluorimetyylikumariini), katekoli-O-metyylitransferaasi (eskuletiini), Glutathioni-S-transferaasi (1-kloori-2,4-dinitrobenseeni).

Tässä kokeessa adenovirukset tai transgeenit eivät aiheuttaneet tilastollisesti merkittäviä muutoksia yhdessäkään näytteessä ($p > 0.05$). Näin ollen adenoviruskäsittely ei todennäköisesti aiheuta muutoksia vierasainemetaboliaan 14 päivän kuluttua käsittelystä.

Acknowledgements

My master's thesis was conducted and completed at the University of Eastern Finland, School of Pharmacy, at the Kuopio campus. I would like to thank my supervisors, professor Jaana Rysä for all the guidance and professor Risto Juvonen for the guidance and planning the experiments that were conducted in the spring 2021. I would also like to thank Hannele Jaatinen for the help preparing the liver samples and Olli Kärkkäinen for the principal component analysis.

Contents

1 Introduction	7
2 Review of the literature	9
2.1 Liver xenobiotic metabolism.....	9
2.1.1 Role of hepatocyte in biotransformation of xenobiotics	10
2.1.2 Drug metabolic enzymes	13
2.1.3 Regulation of xenobiotic metabolism.....	18
2.2 Adenovirus therapies	20
2.2.1 Adenovirus viral vectors.....	21
2.2.2 Adenovirus vector applications	24
3 Aims of the study.....	27
4 Materials and methods	28
4.1 Reagents and chemicals.....	28
4.2 Animals	28
4.3 Preparation of liver samples.....	30
4.4 Viral vectors.....	30
4.5 Drug metabolizing enzyme activity assays	31
4.6 Statistical analysis	37
5 Results	38
5.1 CYP Reactions.....	38
5.2 Conjugation reactions	40
6 Discussion	43
7 Conclusion.....	45
References.....	46

Abbreviations

ABC	ATP-binding cassette
Ad	Adenovirus
AdV	Adenovirus vector
CAR	Coxsackie and adenovirus receptor
CDNB	1-chloro-2,4-dinitrobenzene
COMT	Catechol-O-methyltransferase
CYP	Cytochrome P450
GSH	Glutathione
GST	Glutathione S-transferase
HFC	7-hydroxy-4-trifluoromethylcoumarin
HAd	Human adenovirus
HAdV	Human adenovirus vector
KEAP-1	Kelch-like ECH-related protein 1
Nrf2	Nuclear factor E2 p45-related factor-2
OCA369	3-(3-benzyloxy)-phenyl-7-methoxycoumarin
PAPS	3'-Phosphoadenosine-5'-phosphosulfate
SAM	S-adenosylmethionine
SD-rat	Sprague Dawley rat
SULT	Sulfotransferase
UGT	Uridine 5'-diphospho-glucuronosyltransferase
UDPGA	Uridine-5'-diphospho- α -D-glucuronic acid

1 Introduction

Adenoviruses are an emerging gene transfer tool in the treatment of many types of diseases. These include heritable genetic diseases, various cancers, vaccines like covid-19 and tissue engineering (Lee, C. S. et al. 2017, Ylä-Herttuala and Baker 2017, Lundstrom 2021). Transgene expression caused by adenoviruses is short-lived, which may be desirable depending on the application. Adenoviruses are used because they are capable to transfer large genetic material inside the cell. However, a common cause of failure in gene therapy has been the inefficiency to deliver the transgene into the target cell. (Tilemann et al. 2012).

Viral infections suppress major xenosensors, which leads to decreased expression of xenobiotic-metabolizing enzymes (Huang et al. 2004, Morgan et al. 2008, Klaasen 2019). In animal studies, intravenously administered adenoviruses were targeted in the liver because adenoviruses form complexes with complement component C4-binding protein and blood factor IX, which are then up taken by hepatocytes (Shayakhmetov et al. 2005). This raises the question if metabolic reaction rates of xenobiotics are altered when using adenoviral vectors in gene therapy.

Altered xenobiotic metabolism is relevant in the context of other drug therapies, especially if the drug has narrow therapeutic width. One example of a group of drugs with a narrow therapeutical range is opioids. They may cause adverse effects in case of overdose and if left untreated, the most severe adverse effects lead to death (Terveysportti 2021). Overdose may happen over time even with standard dosing if the metabolic rate of the opioid is significantly decreased. This issue can be overcome with dose adjustments or using an opioid antagonist, however that situation should be avoided in the first place. As opioids are commonly used during cancer treatment, it is plausible that adenoviral vectors and opioids are used at the same time.

A review of the literature of this paper goes through the basics of liver xenobiotic metabolism. This includes various enzymes responsible for catalysing biotransformation reactions, enzymes responsible for the regulation of xenobiotic metabolism, and how molecules pass cell membranes. In the latter section of the review, previous knowledge about adenoviruses is compiled. It contains why adenoviruses are used, the function of adenoviral vectors, and what treatments they are used in. The study of this paper aims to find out if treatment with various recombinant adenovirus transgenes affect xenobiotic-metabolizing enzyme activities in the liver. It was done in vitro xenobiotic metabolism with liver samples acquired from rats after 14 days of treatment with adenoviruses. Enzyme activity was determined by calculating reaction speed from a change of fluorescence in each reaction well over time. Non-fluorescent substrates were converted into fluorescent metabolites or vice versa by different xenobiotic-metabolizing enzymes.

2 Review of the literature

2.1 Liver xenobiotic metabolism

Xenobiotic is a chemical compound that is nutritionally non-essential and does not originate from the organism itself, including pharmaceuticals, naturally occurring compounds, pesticides, etc (National Institutes of Health et al. 2020). The most common route of exposure for xenobiotics is oral and after absorption from the gastrointestinal tract, the portal vein brings them to the liver (Klaasen 2019). One of the many crucial functions of the liver is to metabolize xenobiotic agents to water-soluble and a more readily excreted form, which are metabolites. The liver is the most important tissue where biotransformation of xenobiotics takes place. After biotransformation, metabolites are transferred to blood or excreted into bile, which is then transferred to the intestine. As a result, these metabolites are excreted with feces, unless the metabolite still has attributes that encourage reabsorption. From blood water soluble metabolites are excreted to urine in kidney. Biotransformation reactions are classified by function to oxidation, reduction or hydrolysis (phase 1), or conjugation (phase 2) reactions. Conjugation metabolites with heavy molecular weight xenobiotics such as glucuronide generally improve bile route of excretion, whereas reactions that produce lightweight water-soluble metabolites are typically excreted via kidneys (Figure 1). It is important to note that different species have a high level of divergence in bile excretion and metabolizing enzyme levels (Lin 1995, Klaasen 2019). Therefore, the results of *in vivo* experiments are not directly comparable to humans.

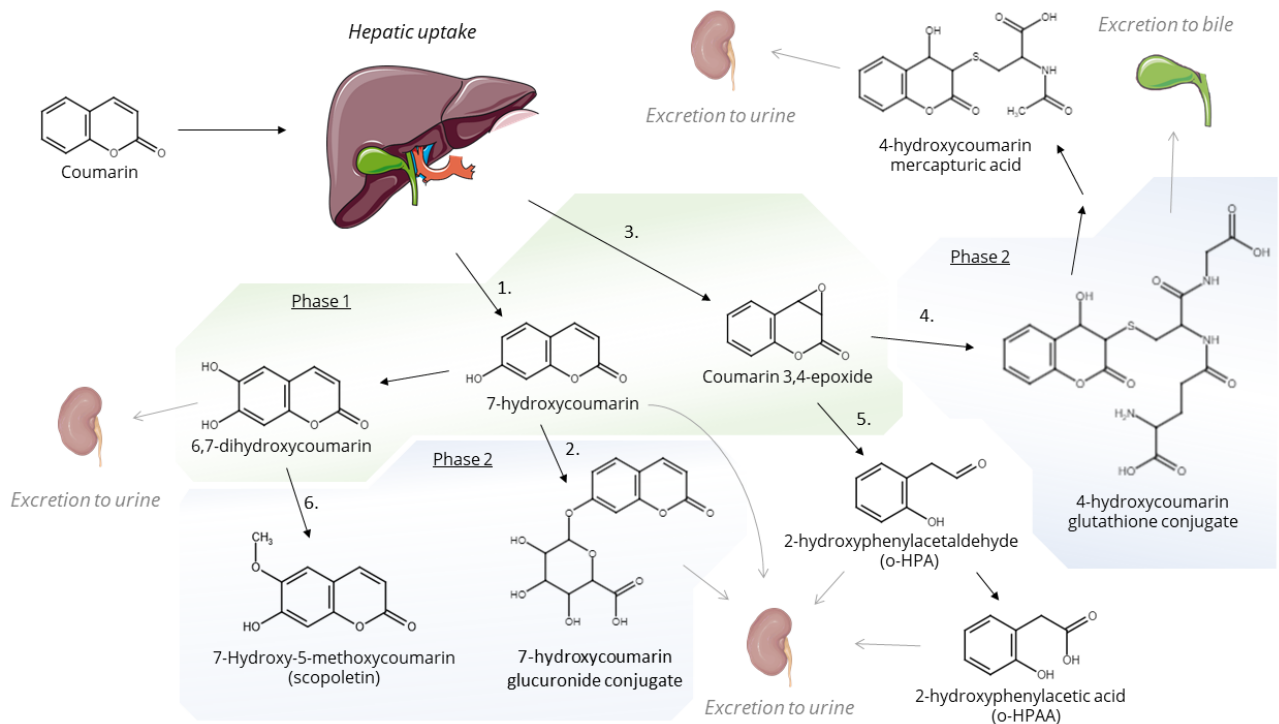


Figure 1. Some coumarin metabolites after phase 1 and phase 2 biotransformation reactions.

1. 7-hydroxylation of coumarin catalysed by human CYP2A6. 2. Glucuronidation of 7-hydroxycoumarin catalysed by UDP-glucuronosyltransferase. 3. 3,4-epoxidation of coumarin catalysed by CYP1A1, CYP1A2, CYP2E1, or CYP3A4. 4. Conjugation of glutathione into coumarin 3,4-epoxide catalysed by glutathione s-transferase. This glutathione conjugate is further metabolized into mercapturic acid. 5. o-HPA is spontaneously hydrolysed from coumarin 3,4-epoxide and is a liver toxic metabolite. 6. 6,7-dihydrocoumarin O-methylation catalysed by catechol-O-methyltransferase. Formed scopoletin is further metabolized to scoparone. Image modified from Lake 1999, Born et al. 2000, and Lewis et al. 2006. The Figure was partly generated using Servier Medical Art, provided by Servier, licensed under a Creative Commons Attribution 3.0 unported license.

2.1.1 Role of hepatocyte in biotransformation of xenobiotics

Hepatocyte cell count is around 60% of the cells in the liver which makes it the most common cell in the liver (Klaasen 2019). Their diameter is about 20-30 μm and they form layers of one to two cells in the liver that are surrounded by canaliculi and sinusoids (Ranta et al. 2017).

Hepatocytes are strongly polarized cells, meaning their basolateral cell membrane has more surface area than the lateral membrane. A larger surface area translates into better uptake of xenobiotics from the bloodstream. The main function of the hepatocytes is to uptake and clear the circulation from environmental toxic compounds, toxins with a dietary origin, and pharmaceuticals (Klaasen 2019). These xenobiotic compounds are transported either passively or actively to hepatocytes. After passing the cell membrane, they are transformed by different enzymes to increase polarity and to make them less toxic. Metabolites formed from the xenobiotics are transferred out of the hepatocyte back to the circulation or to the bile mostly by transporters and then excreted through kidneys or feces. Exposure to a xenobiotic in a whole organism is variably decreased because of the differences in the first-pass metabolism. Hepatocytes are important for metabolic homeostasis, thus disruption in their normal function might be harmful.

Active transport of xenobiotic compounds is used if the xenobiotic is not able to pass through cell membranes passively due to size or insolubility in lipids (Ranta et al. 2017, Klaasen 2019). Facilitated transport does not expend energy whereas active transport does. These xenobiotics are commonly transported through the cell membrane via influx or efflux transporter proteins, which belong to translocase enzymes (EC 7) in Enzyme nomenclature (IUBMB 2022). The most important drug transporters are in the solute carrier (SLC)22A family, which transports cationic and anionic organic compounds and the SLCO transporter family handles amphipathic compounds and larger anions (Ranta et al. 2017). Organic anion and cation-transporting proteins are seen mostly as influx pumps though solutes can move in both directions. Cation pumps use an electrochemical gradient as the driving force of diffusion, whereas anion pumps exploit the exchange of intracellular dicarboxylates to transport substrates against the electrochemical gradient (Klaasen 2019). ATP-binding cassette (ABC) transporter protein is a large superfamily, many of the transporters it includes are important in the homeostasis of various endogenous substrates. P-glycoprotein providing multi-drug resistance ability for cells was the first recognized efflux transporter of the ABC class. ABCC is a subfamily of ABC, that contains transporters like multidrug resistance-associated proteins 2 and 3, which are essential in the efflux of xenobiotics. To get the energy required for their substrate transport through the cell membrane, ABC transporters generally

use up ATP by hydrolysis or binding. ABC transporters have a significant part in absorption from the gastrointestinal tract and elimination to the bile or urine for numerous xenobiotics, and they are expressed in a wide range of cells. Furthermore, the liver and kidney express a special solute carrier family called the multidrug and toxin extrusion transporters, which are responsible for cation efflux out of the cells.

Xenobiotic compounds that can pass through cell membranes passively due to their characteristics, follow Fick's law (Klaasen 2019). It determines that chemicals move from higher concentration to lower without the need for energy. Hydrophobic xenobiotics simply pass the lipid membrane with passive diffusion and small hydrophilic xenobiotics can pass through pores in the membrane. However, the larger the molecule is, the more troublesome it is to pass the membrane via the pores. The rate of membrane passage for larger xenobiotics is dependent on the lipophilicity of the molecule. Furthermore, ionization has an important role in the membrane passage of weak organic bases and acids (Ranta et al. 2017). The ionized form has an electric charge that typically makes the molecule more lipophobic and impedes the passive membrane passage. In contrast, the nonionized form can diffuse through the membrane if other characteristics support the diffusion.

Hepatocytes have so-called xenosensors that are activated by xenobiotics binding to them (Klaasen 2019). These xenosensor proteins affect metabolic enzyme expression by increasing the expression when the enzyme-substrate is present in an elevated concentration. An increase in enzyme expression reverts to normal levels in delay after the xenobiotic concentration decreases. In general, CYP enzyme expression is increased more than the expression of other biotransformation enzyme groups. Notable xenosensors are aryl hydrocarbon receptor (AhR), constitutive androstane receptor, pregnane X receptor (PXR), and peroxisome proliferator-activated receptor α (PPAR α). Binding of inducing xenobiotic to these xenosensors increase different CYP enzyme levels, with some overlap between them. This is due to the same ligands activating multiple xenosensors or different xenosensors and they induce the expression of the same enzymes. Additionally, xenosensors can be activated by endogenous compounds as they have a part in endobiotic homeostasis. Enzymes KEAP-1 and Nrf2 respond to oxidative stress and increase the expression of enzymes that metabolize

electrophiles and reactive oxygen species generating metabolites. Enzymes that decrease oxidative stress include, for example, glutathione transferase, microsomal epoxide hydrolase, aldo-ketoreductase, and aflatoxin aldehyde B1 reductases 1 and 2 (Klaasen 2019).

2.1.2 Drug metabolic enzymes

In general, enzymatic reactions produce more stable and water-soluble products than the original substrate was (Ranta et al. 2017). Usually, these metabolites are less active but, in some cases, like valaciclovir they are more active. Numerous different metabolic enzymes expressed in different tissues can be organized into four classes based on the reaction type they catalyze. These classes are hydrolysis, reduction, oxidation, and conjugation enzymes. Phase 1 reactions, like oxidation, reduction, and hydrolysis transforms a xenobiotic structure in a way that makes it more water-soluble and decreases cell membrane permeability. Cell membrane permeability decreases because a more electronegative functional group is uncovered or added to the xenobiotic by phase 1 enzymes. Conjugation reactions, so-called phase 2 reactions need a nucleophilic or an electrophilic functional group in a xenobiotic, which may be present originally or emerged through a phase 1 reaction (Tukey, R. H. and Strassburg 2000, Fisher et al. 2001, Murphy and Zarini 2002, Klaasen 2019). Phase 2 reactions usually increase hydrophilicity and in general, these reactions decrease xenobiotic toxicity. Any enzyme that catalyses the biotransformation of a xenobiotic can increase the toxicity of some compounds. Fat-soluble or highly permeable xenobiotics that efficiently pass cell membranes with passive diffusion and have a low rate of biotransformation aren't eliminated from an organism in a sufficient time. This is due to reabsorption from the kidneys or intestine. Therefore, a xenobiotic will linger longer in the body and has high exposure to the organism. This might be problematic if the xenobiotic causes undesired effects. On the other hand, excessive metabolic rate causes low exposure, thus desired effects might not be achieved in drug therapy. In other words, disruption in metabolic enzyme function, or their amount might be harmful.

CYP enzymes can catalyze metabolic reactions of numerous xenobiotics and are found in all tissues, however, they are the most abundant in liver microsomes (endoplasmic reticulum)

(Klaasen 2019). They react with various chemical groups, for example, most pharmaceuticals, environmental toxins, industrial, and endogenous compounds (Ranta et al. 2017). CYP enzymes catalyze monooxygenation reactions. One oxygen atom from O_2 is integrated into the substrate and the other is reduced to water by converting NADPH and H^+ into $NADP^+$ (Klaasen 2019). During catalysis, the CYP enzyme does not directly receive electrons from NADPH or NADH, however, it binds the substrate and activates oxygen molecule. The subcellular location of the enzyme determines how it does receive electrons. For example, NADPH-cytochrome P450 reductase protein delivers the electrons from NADPH to the CYP enzyme in the endoplasmic reticulum. To illustrate CYP enzymes catalyzed reaction, below is an example of coumarin hydroxylation (Figure 2).

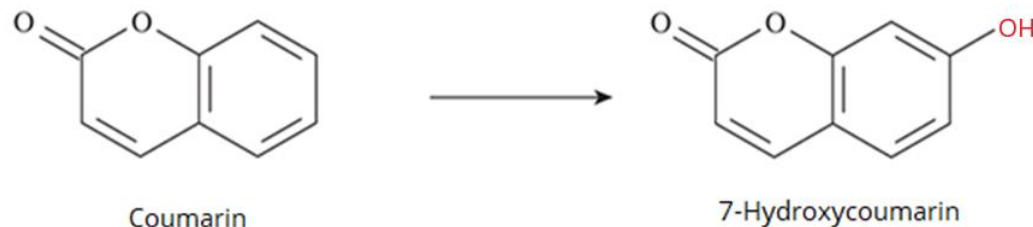


Figure 2. Oxidation reaction of coumarin to 7-hydroxycoumarin by CYP (human CYP2A6). Image modified from Klaasen 2019.

The active site of CYP1A1, CYP1A2, and CYP1B1 is narrow, and suitable only for planar substrates (Feng et al. 2021). They commonly accept polycyclic aromatic hydrocarbons like benzo[a]pyrene and a probe substrate 7-ethoxyresorufin that was used in this study. CYP1A2 is found mainly in the liver and the subfamily of CYP1A is important in the metabolic activation of carcinogens and drug metabolism of various drugs like clozapine, which has narrow therapeutic width. Enzymes of CYP2 family has more variation in the substrate-binding sites and the probe substrate used in this study was 7-pentoxyresorufin for CYP2B. CYP2A6 has a small active site that accepts substrates like coumarin and nicotine whereas CYP2C9 has a medium-size active site for substrates like warfarin and phenytoin (Feng et al. 2021). Like CYP1, the CYP2 family is also found in the liver and is important for the metabolism of drugs. CYP2C9 is involved in the metabolism of 20-30% of drugs and CYP2D6 catalyzes biotransformation reactions for about 20% of drugs. CYP3A family has a large active site that accepts a wide variety of xenobiotics and more than 50%

of the commercial drugs. These include amiodarone, carbamazepine, and midazolam. Like other CYP enzymes, CYP3A4 and CYP3A5 are found mainly in the liver. Their enzyme amount and activity may be changed by other drugs, therefore drug interactions are a common.

In conjugation reactions, endogenous molecule is incorporated into the electrophilic or nucleophilic functional group of xenobiotics (Ranta et al. 2017). These functional groups are present in the molecule, exposed or integrated by other metabolic reactions like phase 1 reactions. The group of conjugation reactions consists of glutathione conjugation, methylation, acetylation, sulfonation, glucuronidation, and coenzyme A mediated conjugation with taurine, glycine, and glutamine, which are amino acids (Figure 3). In general, conjugation reactions increase xenobiotics hydrophilicity and total polar surface area to increase excretion. Methylation and acetylation conjugation reactions are an exception to this rule as they have an opposite effect (Klaasen 2019). These reactions usually decrease toxicity. In some cases, reactive metabolites like carbonium ions may form, which leads to toxicity. Conjugation enzymes are mostly located in the cytosol of the cell with the oddity of UDP-glucuronosyltransferases, which localize in endoplasmic reticulum.

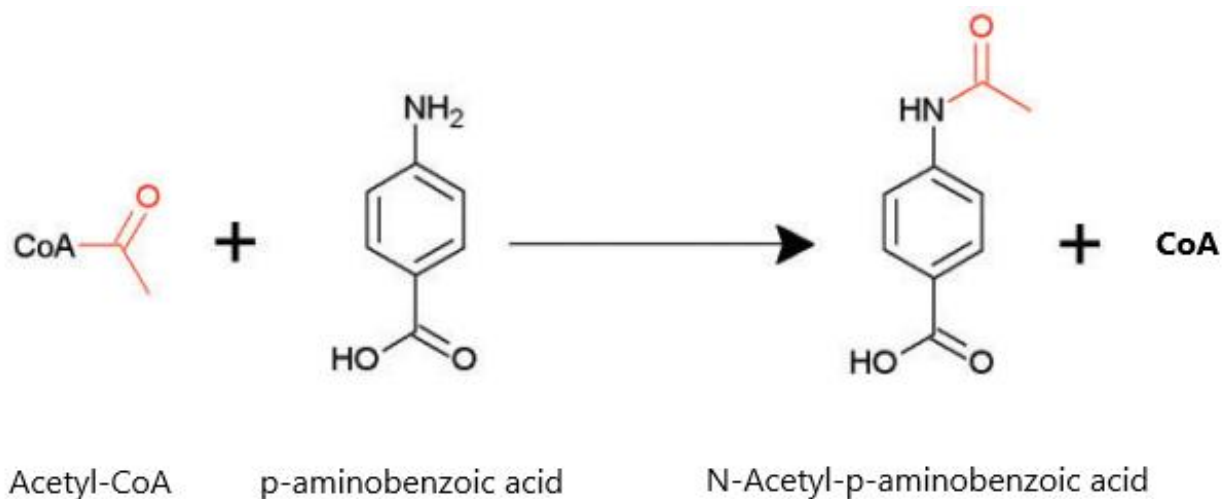


Figure 3. Acetylation of p-aminobenzoic acid. Image modified from Sim et al. 2014.

The uridine 5'-diphospho-glucuronosyltransferase (UGT) family is a significant conjugating enzyme (Tukey, Robert and Strassburg 2000). Uridine-5'-diphospho- α -D-glucuronic acid (UDPGA) releases a glucuronide group that is transferred into the substrate with the help of UGTs. Substrates are various endogenous or xenobiotic compounds. Glucuronide metabolites

are water-soluble and therefore they are readily excreted into the urine. UGTs are mainly found in the liver, but also in the kidney and other tissues (Klaasen 2019). Glucuronidation is a substitution reaction that commonly takes place in nucleophilic groups of the molecule, which are usually N, O, or S heteroatoms. Suitable substrates are usually small and contain an alcohol group, a carboxylic acid, a sulfhydryl group, a primary amine, or a secondary amine. O-sulfonation is a reaction that may happen to substrates that are subject also to O-glucuronidation (Klaasen 2019). Due to this phenomenon, 7-hydroxy-4-trifluoromethylcoumarin was used as a probe substrate for both glucuronidation and sulfonation pathways by changing the available cofactor. 3'-phosphoadenosine 5'-phosphosulfate (PAPS) releases a sulfonate and it is conjugated into the metabolite with the help of sulfotransferases (SULT). These enzymes are found in cytosol of cells all around the body. Unlike UDPGA of the glucuronidation pathway, the amount of PAPS is limited in the body. Therefore, sulfonation reactions are saturated easily, however, they have high affinity. The substrate-binding site of SULTs in the Golgi device accepts hydrophilic carbohydrates, whereas cytosolic SULTs accept small hydrophobic molecules, like catecholamines and phenols (Rath et al. 2004).

Catechol-O-methyltransferase (COMT) pathway is a lesser member of xenobiotic metabolism (Klaasen 2019). As mentioned before, in general methylation of the compound decreases total polar surface area and slightly increases lipophilicity by introducing a methyl group into the molecule with the help of COMT. S-adenosylmethionine works as a cofactor in the reaction and releases the methyl group. Methyl group is attached to electron-rich heteroatoms found in -OH, -SH, and -NH₂ groups and prevents further metabolism, possibly impairing metabolic activation of toxic compounds. COMT substrates are commonly catechol drugs and catecholamine neurotransmitters. In this study, esculetin was used as a probe substrate to determine COMT activity.

Glutathione S-transferase (GST) has a different function compared to the previous conjugating enzymes (Klaasen 2019). Substrates for GST are numerous and electrophilic xenobiotics or their electrophilic metabolites. 1-chloro-2,4-dinitrobenzene (CDNB) was used as a probe substrate for GST in this study. GSTs transfer glutathione (GSH) into electrophilic site of the

molecule (Klaasen 2019). Targets are commonly reactive oxygen species (ROS), therefore GST cuts down oxidative stress. ROS cause lipid peroxidation, protein damage, mutagenic alterations of DNA, and double helix breaks (Juan et al. 2021). Excess oxidative stress caused by xenobiotics may start the development of various diseases including cancer.

Biotransformation of some xenobiotics generates ROS e.g., in uncoupling xenobiotic oxidation reactions of CYPs (Klaasen 2019). Another example, benzo[a]pyrene is oxidized by the P450 enzyme to benzo[a]pyrene-4,5-oxide which is a reactive electrophilic epoxide (Figure 4). Excess amounts of these metabolites can cause cell toxicity and DNA damage. However, the toxic effects of reactive oxygen species and other reactive metabolites are greatly reduced by glutathione (GSH), glutathione S-transferases (GSTs), and glutathione peroxidases. Oxidative stress-reducing and electrophilic metabolites detoxifying enzymes are regulated by GSH levels. As GSH levels decrease, Kelch-like ECH-related protein 1 (KEAP-1) is simultaneously oxidated, which activates nuclear factor E2 p45-related factor-2 (Nrf2), which increases the expression of those enzymes.

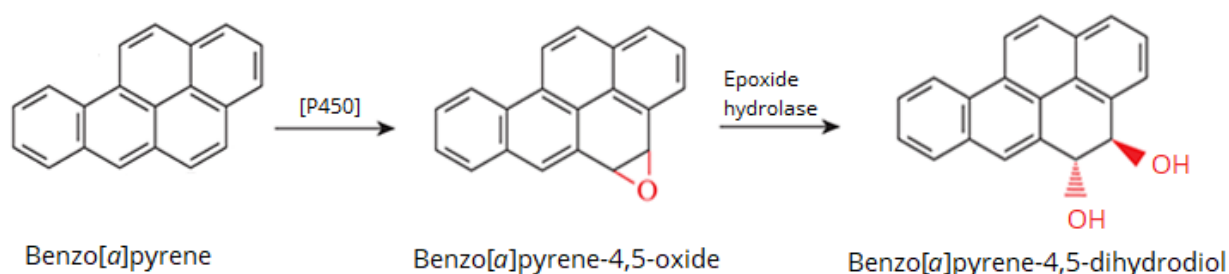


Figure 4. Epoxide hydrolase inactivates electrophilic epoxide generated by CYP (P450) enzyme reactions. Epoxide hydrolysis of benzo[a]pyrene-4,5-oxide to benzo[a]pyrene-4,5-dihydrodiol. Image modified from Klaasen 2019.

Even though the liver is the main organ that handles xenobiotic metabolism, biotransformation activity is also present in other tissues (Klaasen 2019). Azo- and nitro reduction reactions are commonly catalyzed in the lower intestine as an absence of oxygen creates good conditions for these reactions. (Figure 5). In some cases, these biotransformations may be detrimental to the body to get rid of a xenobiotic. Compounds like

2,6-dinitrotoluene go through nitro-reduction to amines by gut microbiota and are activated by metabolism to cause tumours in rat liver (Long and Rickert 1982, Klaasen 2019).

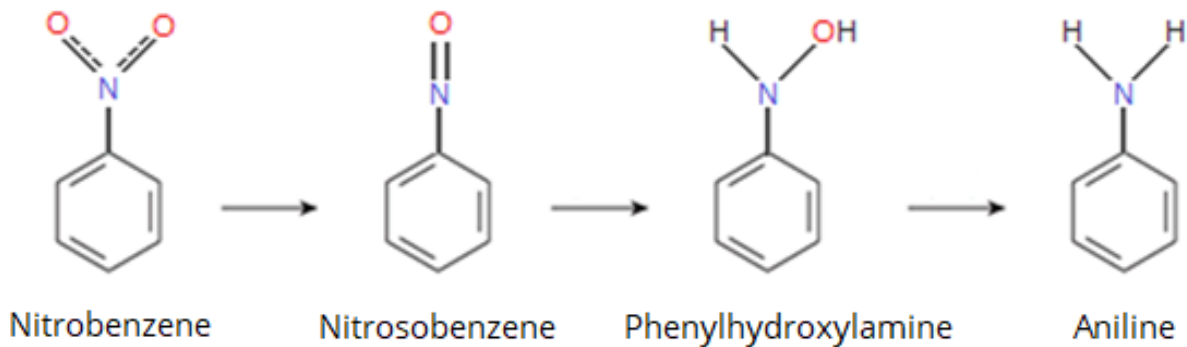


Figure 5. Nitro-reduction reaction chain of nitrobenzene to aniline. Image modified from Klaasen 2019.

2.1.3 Regulation of xenobiotic metabolism

Xenobiotic metabolic elimination correlates with its xenobiotic-metabolizing enzyme activity. Factors that influence basal activity are the amount of the protein and the enzymes' capability to catalyze metabolic reactions. Enzyme activity or expression may be increased or decreased due to exposure to xenobiotics or at diseases (Klaasen 2019). Xenobiotics bind to different xenosensors, and each sensor regulates the expression of a group of xenobiotic-metabolizing enzymes. Their higher concentration and binding to xenosensor leads to higher enzyme expression, thus metabolic rate increases. In addition to this, a xenobiotic can induce other enzymes that affect other xenobiotics.

Upregulation of xenobiotic-metabolizing enzymes may lead to decreased plasma concentrations of drugs, however in the case of metabolic activation concentration of the active metabolite increases (Goodman et al. 2011). After a ligand binds to a xenosensor in the cytosol, for example, the pregnane X receptor (PXR), the PXR forms a complex with the retinoid X receptor. This complex relocates into the nucleus and binds to the DNA, upstream of its target gene. The coactivator gets called up and binds to the TATA box binding protein,

which activates RNA polymerase II and the target gene is transcribed into an active protein. Xenosensor aryl hydrocarbon receptor (AhR) induces CYP1A1, CYP1A2, and CYP1B1 enzymes. As these enzymes may activate chemical carcinogens, AhR induction may lead to an increased amount of procarcinogens. Pregnane X receptor is known to induce the CYP3A4 enzyme, which metabolizes a wide variety of xenobiotics. Among other enzymes, PXR also induces UGTs and SULTs. Constitutive androstane receptor induces CYP2B6, CYP2C9, and CYP3A4, many phase 2 metabolic enzymes that include UGTs, SULTs, and GSTs (Goodman et al. 2011). Peroxisome proliferator-activated receptor α (PPAR α) induces CYP4 enzymes responsible for the oxidation of fatty acids and drugs with fatty acids among other enzymes with similar tasks, A single xenosensor can activate multiple genes that regulate the transcription of xenobiotic-metabolizing enzymes. As there is a lot of overlap between the target genes for different xenosensors, especially for UGTs, a single xenobiotic can affect the metabolism of multiple compounds.

A decrease in enzyme activity has been observed with bacterial and viral infections, vaccinations, inflammatory diseases, cancer, and treatment with specific proinflammatory therapeutic proteins. Nuclear factor kappa-B activated by the diseases mentioned above suppresses all four major xenosensors among other nuclear receptors (Huang et al. 2004, Morgan et al. 2008, Klaasen 2019). Due to this suppression, xenobiotic-metabolizing enzyme expression is decreased, thus enzyme activity decreases. Expression and protein levels of pregnane X receptor and constitutive androstane receptor were altered in the presence of the first generation, serotype 5 adenoviral vector (AdV) expressing AdLacZ transgene in mice (Jonsson-Schmunk et al. 2016). The presence of this virus decreased CYP3A catalytic activity by 56% after 48-hours of administration. They also found that activity is not altered, if the integrin-binding arginine-glycine-aspartic acid sequence is removed from the penton base protein of the viral capsid.

Clinical significance of significantly decreased xenobiotic-metabolizing enzyme activity becomes apparent when a patient is treated with a pharmaceutical, that has narrow therapeutic width or causes severe adverse effects on overdose. Additionally, the desired

effect might not be reached if the enzyme activity is increased. Many pharmaceutical compounds have enzyme-mediated biotransformation and as such are susceptible to enzyme activity changes. However, the most susceptible pharmaceutical group that has clinical significance in conjunction with adenovirus treatments is possibly opioids (Alaspää 2021). Oxycodone and fentanyl for example are used as pain medication during cancer treatment and acute overdose causes respiratory depression and coma (Terveysportti 2021). This can lead to death if the condition is not treated with an opioid antagonist like naloxone. Theoretically, if adenoviruses are used in cancer treatment and if the adenoviruses would cause a significant decrease in CYP3A4 and CYP2D6 enzyme activities, exposure to the aforementioned opioids would increase (Lee, C. et al. 2017, Terveysportti 2021). This issue could be overcome with opioid dosage adjustments to prevent too high exposure and observe the patient's condition. Other xenobiotic compounds like chemotherapeutic pharmaceuticals combined with adenovirus treatments could increase their respective adverse effects. However, it is not known if adenoviruses alter enzyme amount or activity of human CYP3A4 enzymes.

2.2 Adenovirus therapies

A viral vector is a versatile tool that could be used to treat e.g. inherited genetic diseases, cancer, and to give vaccinations (Lasaro and Ertl 2009, Lee, C. et al. 2017, Lee, D. et al. 2019). Gene therapy has the possibility of treating the fundamental problem behind a disease instead of symptom treatment. Delivering a transgene non-virally causes the least possible immunogenicity and has a good safety profile, however, this approach suffers from inadequate efficiency to deliver a transgene inside a cell (Tilemann et al. 2012). In general, inefficient gene delivery has been the most hindering cause of in vivo gene therapies. In contrast, viruses are brilliant in releasing their genetic material inside a cell and this trait can be exploited to increase transgene delivery efficiency.

Adenovirus gene therapy has had its fair share of misfortunes during the last decades. Intra-arterial infusion with a high dose caused the death of a patient in experimental treatment in

1999, and the development of leukemia in two patients in 2002 (Buckley 2002, Raper et al. 2003, Lee, C. et al. 2017). These cases raised safety concerns about adenovirus treatments however adenovirus therapies today are a focus of research and a steadily advancing field (Lee, C. et al. 2017). Adenovirus vectors have major advantages in genetic stability, production scalability, and gene transduction capability. Adenoviruses have non-integrative characteristics, and due to inflammation and immune response, protein expression lasts only for weeks, because transgene expressing cells are eventually killed (Bouard et al. 2009, Giacca and Zacchigna 2012). A major disadvantage for adenoviruses is that their capsid may cause an intense immune response (Raper et al. 2003, Lee, C. et al. 2017). However, the immune reaction attribute has been reduced from the third generation of adenoviruses; high-capacity AdVs so-called helper-dependent adenoviruses, or gutless adenoviruses (Parks et al. 1996, Lee, C. et al. 2017). These viruses do not have viral genetic components or vital packaging proteins. The viral proteins are produced by helper viruses that are functioning normally, except their recombinated genome is not packed inside the virus vector. Nevertheless, helper virus contamination is an issue that prevents human use of helper-dependent adenovirus vectors but strategies tackling this issue are being developed further. Properties between different virus vectors or non-viral delivery methods are not described in this paper but one can find this comparison e.g., from Lee et al. (2017) paper.

2.2.1 Adenovirus viral vectors

Adenoviruses of the C family, that cause e.g., respiratory tract infections, do not cause tumours in humans (Meier and Greber 2003). Due to their capacity to transfer large genomes and efficiency to infect various cell types, human adenoviruses (HAd5) have undergone substantial research. They have an outer capsid with a shape of a relatively large icosahedron (diameter ~95nm), consisting of large polypeptides e.g., the hexon and the penton base, trimeric fibre knob proteins, and various other proteins (Figure 6) (Rux and Burnett 2004, Gallardo et al. 2021). Inside the adenovirus capsid, the genome is linear double-stranded DNA of 36 000 base pairs with proteins packing the DNA to a smaller volume among other proteins.

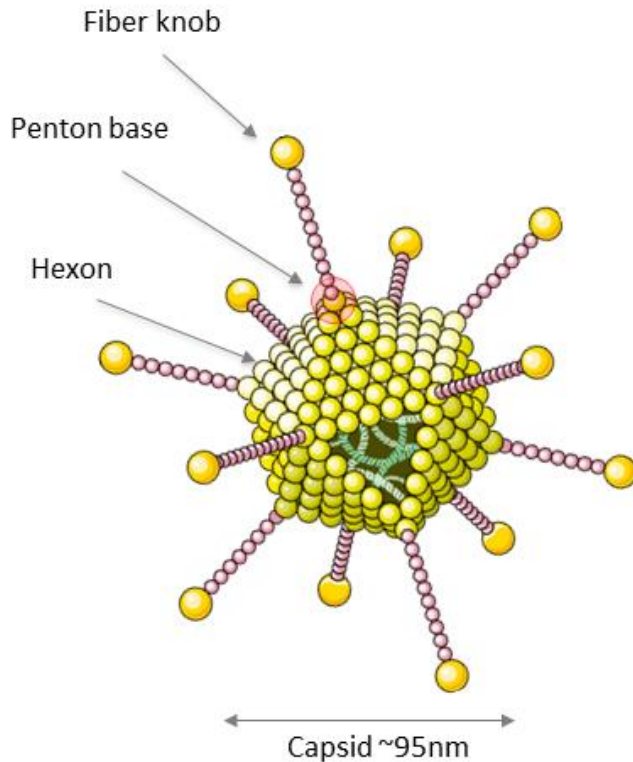


Figure 6. Structure of an adenovirus. Figure modified from Rux and Burnett (2004) and was generated using Servier Medical Art, provided by Servier, licensed under a Creative Commons Attribution 3.0 unported license.

HAdVs have fibres sticking out on the surface of the capsid and the fibres are attached to the penton base protein (Stasiak and Stehle 2020). The head of the fibre has a complex that is capable to interact with various receptors of the target cell (Bergelson et al. 1997, Bewley et al. 1999, Marttila et al. 2005, Wang et al. 2011, Willison et al. 2011, Lenman et al. 2018, Stasiak and Stehle 2020). These receptors include Coxsackie and Adenovirus Receptor (CAR), desmoglein-2, CD46, polysialic acid, and GD1a glycan receptor among other receptors making HAdV competent in infecting various cells. After binding fibres to the cell integrin transmembrane receptors, typically CAR and α_v integrin, fibres are mechanically plucked out of the penton base (Nemerow and Stewart 2016). This is due to the fibre-penton base bond being weaker than the fibre receptor bond. The penton base protein has a loop, that interacts with various integrin receptors, thus triggering and exploiting several signalling pathways to provoke endocytosis and macropinocytosis. As a result, the virus enters the cell (Figure 7).

Adenoviruses have an extraordinary quantity of DNA-binding proteins with viral origin inside the protein capsid, which is a unique trait of the adenoviruses (Gallardo et al. 2021).

Adenoviruses undergo maturation process, where a viral protease cleaves several proteins of the virus, thus increasing pressure inside the capsid (Pérez-Berná et al. 2009, Pérez-Berná et al. 2012, Ortega-Esteban, A. et al. 2013, Ortega-Esteban, Alvaro et al. 2015, Gallardo et al. 2021). Studies show that this is likely due to electrostatic repulsion change with the DNA and other viral proteins. Increased pressure works like a primer for the adenovirus particle disassembly. Capsid disassembly is theorized to begin because of the fibre proteins being plucked out of the penton base by fibre-integrin receptor interactions (Burckhardt et al. 2011, Nemerow and Stewart 2016). The penton bases interacting with integrin receptors as mentioned before, additionally cause conformational changes in the penton bases, destabilizing the capsid. Together, the increased pressure causes mechanical stress on the capsid, fibre release, and penton base-integrin interaction causes the capsid to burst open, exposing the DNA that is still connected to the pieces of the capsid (Figure 7).

Successful infection requires translocation of the viral genome to the cytosol of the host cell. When the adenovirus capsid is disassembled, protein VI found inside the capsid is exposed (Wiethoff et al. 2005). Wiethoff et al. did show that protein VI causes nonspecific disruption in lipid membranes, thus enabling the release of the viral genome into the cytosol of the host cell. Furthermore, after cytoplasmic transport to the nucleus, the nuclear pore complex functions as a dock for the adenovirus particle (Greber et al. 1997). Following the docking of the virus, the adenovirus capsid is disassembled. Viral DNA is detached from the capsid and inserted into the nucleus via the same nucleus pore complex (Figure 7).

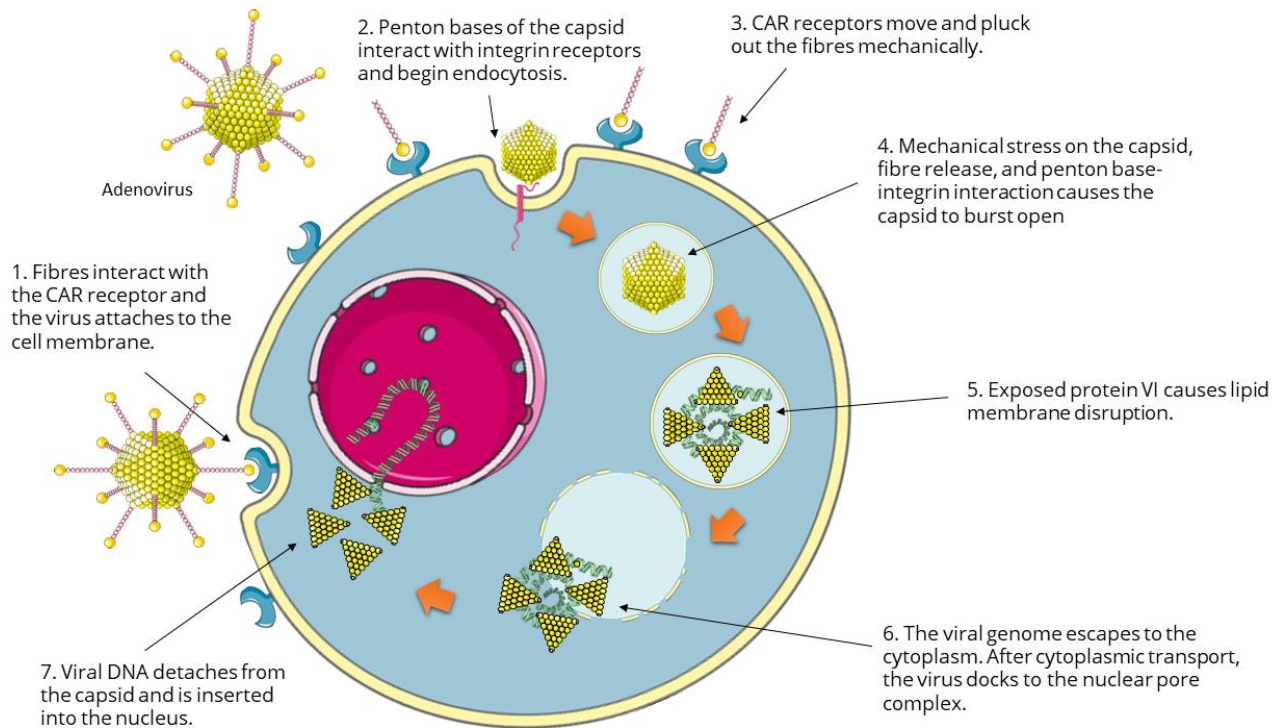


Figure 7. Process of the adenovirus infection as described in the previous text. Fibres bind to the coxsackie and adenovirus receptor, and the virus breaches into the cell. The capsid bursts open, and the virus escapes to the cytosol. Finally, the viral DNA enters the nucleus. The figure was drawn using pictures from Servier Medical Art. Servier Medical Art by Servier is licensed under a Creative Commons Attribution 3.0 Unported License.

Adenoviruses are targeted in the liver because the fibre knob of the virus can bind to coagulation factor IX and complement component C4-binding protein (Shayakhmetov et al. 2005). This complex is up taken by hepatocytes in mice and nonhuman primates when adenoviruses are administered intravenously. As viral infections decrease enzyme activity, it raises the question if viral vectors alter liver metabolic activity (Klaasen 2019).

2.2.2 Adenovirus vector applications

During the last decades, numerous applications for adenovirus vectors have been developed. Some of them have failed, some have succeeded, and many are under development or clinical trials. These various applications include anticancer therapies, monogenic disease therapies,

bone tissue regeneration, heart failure, and vaccines like covid-19 (Lee, C. et al. 2017, Ylä-Herttuala and Baker 2017, Lundstrom 2021). Two of the covid-19 vaccines used in Finland were based on adenoviral vectors (Finnish institute for health and welfare 2022). These were Jcovden by Janssen and Vaxzevria by Astra Zeneca. Jcovden is based on a replication-incompetent human adenovirus type 26 (Ad26) vector, which contains a transgene that encodes a SARS-CoV-2 spike (S) protein in a stabilized conformation (EMA 2022a). Respectively, Vaxzevria is based on Chimpanzee Adenovirus encoding the SARS-CoV-2 Spike glycoprotein ChAdOx1-S (EMA 2022b). Below is a table of some plausible adenovirus vector applications (Table 1). Furthermore, adeno-associated viruses are studied for the treatment of hyperlipidemias, atherosclerosis, and lipoprotein metabolism (Ylä-Herttuala and Baker 2017). Numerous cardiovascular gene therapy clinical trials have been suffering from a lack of efficiency or detectable effects due to e.g., dose optimization, gene transfer efficiency, insufficient vector distribution, and short half-life.

Table 1. Examples of plausible adenovirus vector applications.

Therapy	Application	Vector	Mechanism of action
Mono-genic disease therapy	Alpha-1 antitrypsin deficiency	AdV containing A1AT transgene	Introduce alpha-1 antitrypsin for its deficiency
Anti-cancer therapy	Colorectal cancer, hepatocellular carcinoma, non-small cell lung cancer, prostate cancer, breast cancer, ovarian cancer, glioma, advanced and unresectable cancers, etc.	Replication-defective AdV (Advexin, Gendicine) Replication-competent AdV (ONYX-015, Oncorine)	Induce antitumoral immune response Cause oncolysis Both may be used to deliver or overexpress tumor suppressor genes (e.g., p53), cytotoxic genes, cause cell cycle arrest or trigger apoptosis.
Vaccines	HIV, Ebola, Covid-19	AdV containing one or several pathogen protein transgenes	A potent cytotoxic T-cell response that is effective for intracellular pathogens, and antibody-mediated immunity response
Regenerative medicine	Bone tissue engineering, bone regeneration	AdV containing transgenes for osteoinductive growth factors	The purpose of bone tissue engineering is to activate osteogenic differentiation, promote ossification and unification with surrounding bone tissue

3 Aims of the study

This study aimed to find out if recombinant adenovirus transgenes cause alteration in xenobiotic metabolic enzyme activities in rat liver. Because intravenously administered AdVs are targeted into the liver in mice, and viral infections decrease enzyme activity a decrease in metabolic enzyme activity is expected (Shayakhmetov et al. 2005, Klaasen 2019). Previous studies have found that a vector without a transgene might cause a decrease in enzyme activity (Callahan et al. 2008). This suggests that all viruses studied this time should decrease metabolic activity unless the transgene they are carrying is somehow able to counteract this effect. If mRNA levels for the enzyme would be elevated, enzyme expression should still decrease, because hepatocytes might be focused on producing viral transgene products (Jonsson-Schmunk et al. 2016). Normal variation of CYP enzyme concentrations between individuals can range 2-36 -fold, therefore changes of less than -50% to 100% have minimal biological significance (Snawder and Lipscomb 2000).

4 Materials and methods

4.1 Reagents and chemicals

7-Pentoxoresorufin, esculetin, scopoletin, PAPS, alamethicin, Uridine-5'-diphospho- α -D-glucuronic sodium salt (UDPGA), NADP⁺, and 7-hydroxy-4-trifluoromethylcoumarin (HFC) were acquired from Sigma-Aldrich (Mannheim, Germany). 7-Ethoxoresorufin, isocitric acid dehydrogenase, isocitric acid, MnCl₂, MgCl₂, chlorodinitrobenzol (CDNB, $\geq 99\%$, arrived 11.3.2009), and reduced L-glutathione (GSH, opened 14.9.2018) were acquired from Sigma-Aldrich (Steinheim, Germany). BioRad reagents were bought from Bio-Rad Laboratories, Inc. KCl were obtained from J.T. Baker (Deventer, The Netherlands). Milli-Q Gradient A10 deionized water was used in all experiments. NADPH regenerating system were made from 188 mM Tris-HCl buffer solution, 16.8 mM isocitric acid, 12.5 mM MnCl₂, 12.5 mM MgCl₂, 1.12 mM NADP⁺, 0.056 mM KCl, and 15 U isocitric acid dehydrogenase, pH 7.4. Other solutions used were K-phosphate buffer and DMSO in water.

4.2 Animals

Male 2-to-3-month-old Sprague-Dawley (SD) rats weighing 250-300 g from the colony of the Center of Experimental Animals at the University of Oulu, Finland, were used. All rats were kept in plastic cages with free access to tap water and regular rat chow in a room with a controlled 40 % humidity and a temperature of 22 °C. A 12 h light and 12 h dark environmental light cycle was maintained.

All experimental protocols were approved by the Animal Use and Care Committee of the University of Oulu and the Provincial Government of Southern Finland, Department of Social Affairs and Health, Finland. The study conforms to the Guide for the Care and Use of Laboratory Animals published by the US National Institutes of Health.

Adenovirus gene transfer

Male Sprague-Dawley rats (n=2-7 per group) were anaesthetized with medetomidine hydrochloride (Domitor 250 µg/kg, i.p.) and ketamine hydrochloride (Ketamine 50 mg/kg, i.p.). A left thoracotomy and pericardial incision were made. Adenovirus-mediated gene transfer was performed as previously described (Tenhunen et al. 2006). Adenovirus constructs used in this study are shown in Table 2. After the operation, the anaesthesia was partially antagonized with atipamezole hydrochloride (Antisedan 1.5 mg/kg, i.p.) and the rats were given buprenorphine hydrochloride (Temgesic, 0.05-0.2 mg/kg s.c.) for analgesia. Two weeks after gene delivery, the rats were sacrificed, livers were weighed, and the tissue samples were immersed in liquid nitrogen and stored at -70°C for later analysis.

Table 2. Number of animals at each transgene group. Note that there were four different SD-rat livers, one of the samples was a duplicate.

Gene cassette	Number of samples
SD-rat	5 (4 rats)
NLS-LacZ	7
LacZ	6
Nkx2.5+GATA	6
Nkx2.5	2
ASPEX	3
PEX	3
rSMARCKD3	4

4.3 Preparation of liver samples

At -80 C stored liver samples were thawed and kept on ice during the whole preparation procedure. The samples were randomized, numbered, and approximately 0.5 g sample of each liver was cut off. The liver samples were transferred to bead mill homogenizer tubes with 100 mM Tris-HCL buffer solution, pH 7.4. The amount of the homogenization buffer in ml was two times the mass of the liver sample. After homogenization, the liver samples were transferred to centrifuge tubes, the homogenization vial was washed with one part of 100 mM Tris-HCL buffer pH 7.4 and combined with the homogenate, then centrifuged for 20 minutes at 10 000 x g at 4 C. The supernatant containing microsomes and cytosol was collected and spun for 60 minutes in an ultracentrifuge at 100 000 x g at precooled temperature of 4°C. The supernatant containing cytosol was then transferred to the Eppendorf tube and aliquoted to new tubes. The pellet containing microsomes was suspended with microsomal storing buffer containing 20 % glycerol 500 µl of suspension was added per 500 mg of the cut liver sample. Then suspension aliquots were transferred to tubes. Both microsome and cytosol samples were stored at -80°C until experiments were carried out. Bradford method of Bio-Rad Protein determination was used to measure protein levels of each sample.

4.4 Viral vectors

Drug metabolizing enzyme activities were determined in liver microsomes of rats treated with adenoviruses containing the following gene cassettes: Nkx2.5+GATA, Nkx2.5, ASPEX, PEX, rSMARCD3, NLS-LacZ, and LacZ in recombinant replication-deficient adenovirus type 5 (Ad5). Untreated Sprague Dawley rats acted as a control. Samples of LacZ acted as additional missense controls. Transgenes used and their basic function are shown in Table 3.

Table 3. Transgenes, concentration, and their function.

Name	Plague forming units	Function
LacZ	5×10^9	Gene coding for β -galactosidase
NLS-LacZ	4×10^9	Gene coding for β -galactosidase with nuclear localization signal (NLS)
Nkx2.5	5×10^9	Gene coding NK2 Homeobox 5 (Nkx2.5) transcription factor gene
Nkx2.5 + GATA-4	$5 \times 10^9 + 1 \times 10^9$	Genes coding Nkx2.5 and GATA-4 transcription factors.
PEX	5×10^9	Phenylephrine regulated factor 1 (PEX-1) coding gene
ASPEX	5×10^9	Antisense PEX-1
rSMARCD3	8×10^9	Gene coding SWI/SNF Related, Matrix Associated, Actin Dependent Regulator of Chromatin, Subfamily D, Member 3

4.5 Drug metabolizing enzyme activity assays

Reaction rates of several probe xenobiotic metabolic reactions were measured, including CYP, glucuronidation, sulfonation, catechol-O-methyltransferase methylation (COMT), and GST. End products of the reactions performed in activity assays have different fluorescence (or absorbance in the case of experiment 8) than substrates, therefore measuring change of fluorescence over time can be used to calculate reaction rate (Juvonen et al. 2019, Raunio et al. 2020). Basic principle of coumarin derivative reactions is shown in Figure 8. Incubation conditions and measurements described and summarized below in table 4. NADPH

regenerating system used in experiments 1-4 was composed of 1.12 mM NADP⁺, 12.5 mM MgCl₂, 12.5 mM MnCl₂, 16.8 mM isocitric acid, 0.056 mM KCl, and 15 U isocitric acid dehydrogenase in a 188 mM Tris-HCl buffer, pH 7.4.

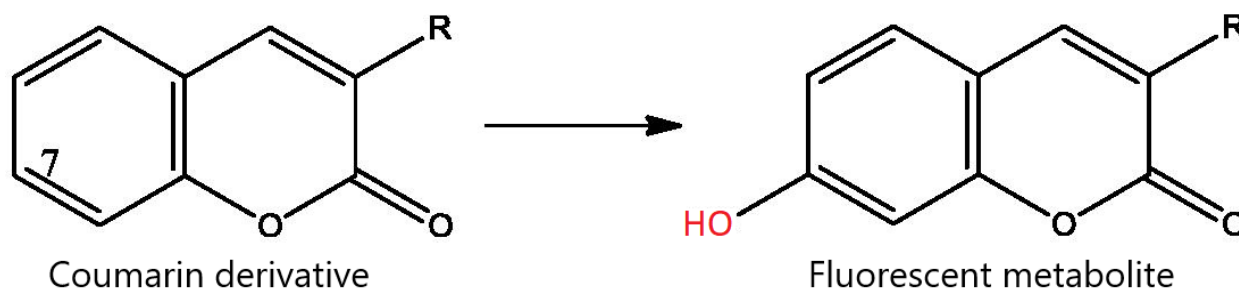


Figure 8. Biotransformation of non-fluorescent coumarin derivative to fluorescent metabolite. Image modified from Juvonen et al. (2019).

In experiment 1, the substrate of CYP1 enzyme family 7-ethoxyresorufin (0.1 μ l of 1 mM solution) was pipetted into a 96 well plate. Activity assay was done in a total volume of 100 μ l, which contained 10 μ l of 100 mM Tris-HCl buffer (pH 7.4), 1 μ l of liver microsomes. 20 μ l of NADPH regenerating system was used to start the reaction. In blank wells, microsomes were replaced with 1 μ l of Milli-Q water. Victor fluorescent plate reader, 96 well plate and all reagents were prewarmed for 5 min at 37°C before measurement. The incubation temperature was 37°C and NADPH was added just before starting measurements. Fluorescence was measured every 2 minutes for 40 minutes period and the plate was automatically shaken between measurements. The excitation filter was set to 570 nm and detection at 615 nm.

In experiment 2, the substrate of CYP2B enzyme family 7-pentoxyresorufin (0.2 μ l of 0.5 mM solution) was pipetted into a 96 well plate. Activity assay was done in a total volume of 100 μ l, which contained 10 μ l of 100 mM Tris-HCl buffer (pH 7.4), 2 of μ l liver microsomes. 20 μ l of NADPH regenerating system was used to start the reaction. In blank wells, microsomes were replaced with 2 μ l of Milli-Q water. Victor fluorescent plate reader, 96 well plate and all reagents were prewarmed for 5 min at 37°C before measurement. The incubation temperature was 37°C and NADPH was added just before starting measurements.

Fluorescence was measured every 2 minutes for 40 minutes period and the plate were automatically shaken between measurements. The excitation filter was set to 570 nm and detection at 615 nm.

In experiment 3, substrate of several CYP enzymes 3-(3-benzyloxy)-phenyl-7-methoxycoumarin (OCA369) (0.1 μ l of 10 mM solution) were pipetted into a 96 well plate. Activity assay was done in a total volume of 100 μ l, which contained 10 μ l of 100 mM buffer (pH 7.4), 2 μ l of liver microsomes. 20 μ l of NADPH regenerating system was used to start the reaction. In blank wells, microsomes were replaced with 2 μ l of Milli-Q water. Victor fluorescent plate reader, a 96 well plate and all reagents were prewarmed for 5 min at 37°C before measurement. Incubation temperature was 37°C and 20 μ l of NADPH regenerating system was used to start the reaction just before starting measurements. Fluorescence was measured every 2 minutes for 40 minutes period and the plate were automatically shaken between measurements. The excitation filter was set to 405 nm and detection was at 460 nm.

In experiment 4, substrate of several CYP enzymes family 7-ethoxycoumarin (0.5 μ l of 10 mM solution) were pipetted into a 96 well plate. Activity assay was done in a total volume of 100 μ l, which contained 10 μ l of 100 mM Tris-HCl buffer (pH 7.4), 2 μ l of liver microsomes. 20 μ l of NADPH regenerating system was used to start the reaction. In blank wells, microsomes were replaced with 2 μ l of Milli-Q water. Victor fluorescent plate reader, a 96 well plate and all reagents were prewarmed for 5 min at 37°C before measurement. Incubation temperature was 37°C and 20 μ l of NADPH regenerating system was added to start the reaction just before measurements. Fluorescence was measured every 2 minutes for 40 minutes period and plate were automatically shaken between measurements. The excitation filter was set to 405 nm and detection was at 460 nm.

In experiment 5, substrate of glucuronidation pathway 7-hydroxy-4-trifluoromethylcoumarin (HFC) (0.1 μ l of 10 mM solution) were pipetted into a 96 well plate. Activity assay was done in a total volume of 100 μ l, which contained 10 μ l of 100 mM K-phosphate buffer (pH 7.4), 1 μ l of liver microsomes, 2.5 μ l of 100 mM MgCl₂, 5 μ l of 0.5 mg/ml alamethicin and 71.4 μ l 10 μ l of 5 mM uridine-5'-diphospho- α -D-glucuronic (UDPGA) was used to start the reaction. In blank

wells, microsomes were replaced with 1 μ l of Milli-Q water. Victor fluorescent plate reader, a 96 well plate and all reagents were prewarmed for 5 min at 37°C before measurement. Incubation temperature was 37°C and 10 μ L 5 mM UDPGA was added just before starting measurements. Fluorescence was measured every 2 minutes for 40 minutes period and plate were automatically shaken between measurements. The excitation filter was set to 405 nm and detection was at 460 nm.

In experiment 6, substrate of sulfonation pathway HFC (0.1 μ l of 10 mM solution) were pipetted into a 96 well plate. Activity assay was done in a total volume of 100 μ l, which contained 10 μ l of 100 mM K-phosphate buffer (pH 7.4), 2.5 μ l of 100 mM $MgCl_2$, 1 μ l of liver cytosol. 10 μ l of 100 mM 3'-phosphoadenosine-5'-phosphosulfate (PAPS) was used to start the reaction. In blank wells, cytosol was replaced with 1 μ l of Milli-Q water. Victor fluorescent plate reader, 96 well plate and all reagents were prewarmed for 5 min at 37°C before measurement. Incubation temperature was 37°C and 10 μ L 100 μ M PAPS was added just before starting measurements. Fluorescence was measured every 2 minutes for 40 minutes period and plate were automatically shaken between measurements. The excitation filter was set to 405 nm and detection was at 460 nm.

In experiment 7, substrate of catechol-O-methyltransferase pathway esculetin (0.1 μ l of 10 mM solution) were pipetted into a 96 well plate. Activity assay was done in a total volume of 100 μ l, which contained 10 μ l of 100 mM K-phosphate buffer (pH 7.4), 5 μ l of 100 mM $MgCl_2$, 1 μ l of liver cytosol, 0.1 μ l of 10 mM esculetin, 10 μ l of 1 mM S-adenosylmethionine was used to start the reaction. In blank wells, cytosol was replaced with 1 μ l of Milli-Q water. Victor fluorescent plate reader, 96 well plate and all reagents were prewarmed for 5 min at 37°C before measurement. Incubation temperature was 37°C and 10 μ L 1 mM SAM was added just before starting measurements. Fluorescence was measured every 2 minutes for 40 minutes period and the plate were automatically shaken between measurements. The excitation filter was set to 405 nm and detection was at 460 nm.

In experiment 8, substrate of glutathione S-transferase pathway 1-chloro-2,4-dinitrobenzene (CDNB) (4 μ l of 50 mM solution) were pipetted into a 96 well plate. Activity assay was done in a

total volume of 200 μ l, which contained 171 μ l of 100 mM K-phosphate buffer (pH 7.4), 5 μ l of liver cytosol, 4 μ l of 50 mM CDNB. 20 μ l of 10 mM glutathione (GSH) was used to start the reaction. In blank wells, cytosol was replaced with 5 μ l of Milli-Q water. Hidex absorbance plate reader, 96 well plate and all reagents were prewarmed for 5 min at 37°C before measurement. Incubation temperature was 37°C and 20 μ L 10 mM GSH starter was added just before starting measurements. Absorbance at 340 nm was measured in intervals of one minute over 20 minutes and the plate was automatically shaken between measurements.

Table 4. Table of reactions and reagents used in different enzyme assays. Concentrations are at incubation conditions.

Experiment number	Studied enzyme	Reaction	Buffer and enzyme source	Substrate and other reagents
1	CYP1	O-deethylation	100 mM Tris-HCl, microsomes	1 μ M 7-ethoxyresorufin, 20 % NADPH regeneration system
2	CYP2B	O-dealkylation	100 mM Tris-HCl, microsomes	1 μ M 7-pentoxyresorufin, 20 % NADPH
3	Several CYP	O-demethylation	100 mM Tris-HCl, microsomes	10 μ M OCA369, 20 % NADPH
4	Several CYP	O-deethylation	100 mM Tris-HCl, microsomes	10 μ M 7-ethoxycoumarin, 20 % NADPH
5	UGT	Glucuronidation	100 mM K-phosphate, microsomes	10 μ M HFC, 2.5 mM MgCl ₂ , 25 μ g/ μ l Alamethicin, 0.5 mM UDPGA
6	SULT	Sulfonation	100 mM K-phosphate, cytosol	10 μ M HFC, 2.5 mM MgCl ₂ , 10 μ M PAPS
7	COMT	O-methylation	100 mM K-phosphate, cytosol	10 μ M Esculetin, 5 mM MgCl ₂ , 100 μ M S-adenosylmethionine, scopoletin (in standards)
8	GST	Glutathione conjugation	100 mM K-phosphate, cytosol	1 mM CDNB in DMSO, 1 mM GSH

4.6 Statistical analysis

Data analysis was done with Microsoft Excel by calculating standard slopes and intercepts at each time point and then converting fluorescence readings to concentration. The concentrations were plotted against the incubation time. Only linear sections from beginning of scatter plot charts were taken into consideration when calculating reaction rates. Unpaired student's t-test with two-tailed t-distribution between individual treatment groups was done with GraphPad 5 prism, alpha level was a commonly used $\alpha=0.05$. Additionally, the Pearson correlation matrix for experiments 1-4 and 5-8 was done with GraphPad 5 prism.

5 Results

5.1 CYP Reactions

Experiment 1 (7-ethoxyresorufin) measuring CYP1 enzyme family oxidation reactions did not show significant differences between the groups (Figure 9). There was some increase in the average reaction rate of the PEX compared to SD-rat control (an increase of 132%), however, the PEX group had a wide 95% confidence interval, and the difference was not statistically significant ($p=0.0925$, $p>0.05$). 7-Ethoxyresorufin O-deethylase activity did not show correlation with 7-pentoxyresorufin O-dealkylation ($r=0.229$), oxidation of OCA369 ($r=0.021$), or 7-ethoxycoumarin O-deethylation activities ($r=0.170$) (correlation figures are not shown).

Experiment 2 (7-pentoxyresorufin) measuring CYP2B enzyme family oxidation reactions did not show significant differences between the groups (Figure 9). The largest difference between averages was observed in the treatment group Nkx2.5 and the control (decrease of 40%). However, the Nkx2.5 group has only two samples, therefore this is likely due to random error and the difference is not statistically significant ($p=0.2841$, $p>0.05$). 7-pentoxyresorufin O-dealkylation did show moderate correlation with oxidation of OCA369 ($r=0.513$), and strong correlation with oxidation of 7-ethoxycoumarin ($r=0.781$) (correlation figures are not shown).

Experiment 3 (OCA369) measuring several CYP enzyme family oxidation reactions did not show significant differences between the groups (Figure 9). The largest difference between averages was observed in the treatment group Nkx2.5+GATA compared to the control (a decrease of 26%). However, the 95% confidence intervals have significant overlap. Additionally, this was not a statistically significant finding ($p=0.0617$, $p>0.05$). OCA369 O-demethylation did show somewhat strong correlation with O-deethylation of 7-ethoxycoumarin ($r=0.611$) (correlation figures are not shown).

Experiment 4 (7-ethoxycoumarin) measuring several CYP enzyme family oxidation reactions did not show significant differences between the groups (Figure 9). The largest difference in

reaction rate averages was observed between treatment groups Nkx2.5 and the control (a decrease of 45%). However, the Nkx2.5 group has only two samples, therefore this is likely due to random error and the difference is not statistically significant ($p=0.2627$, $p>0.05$).

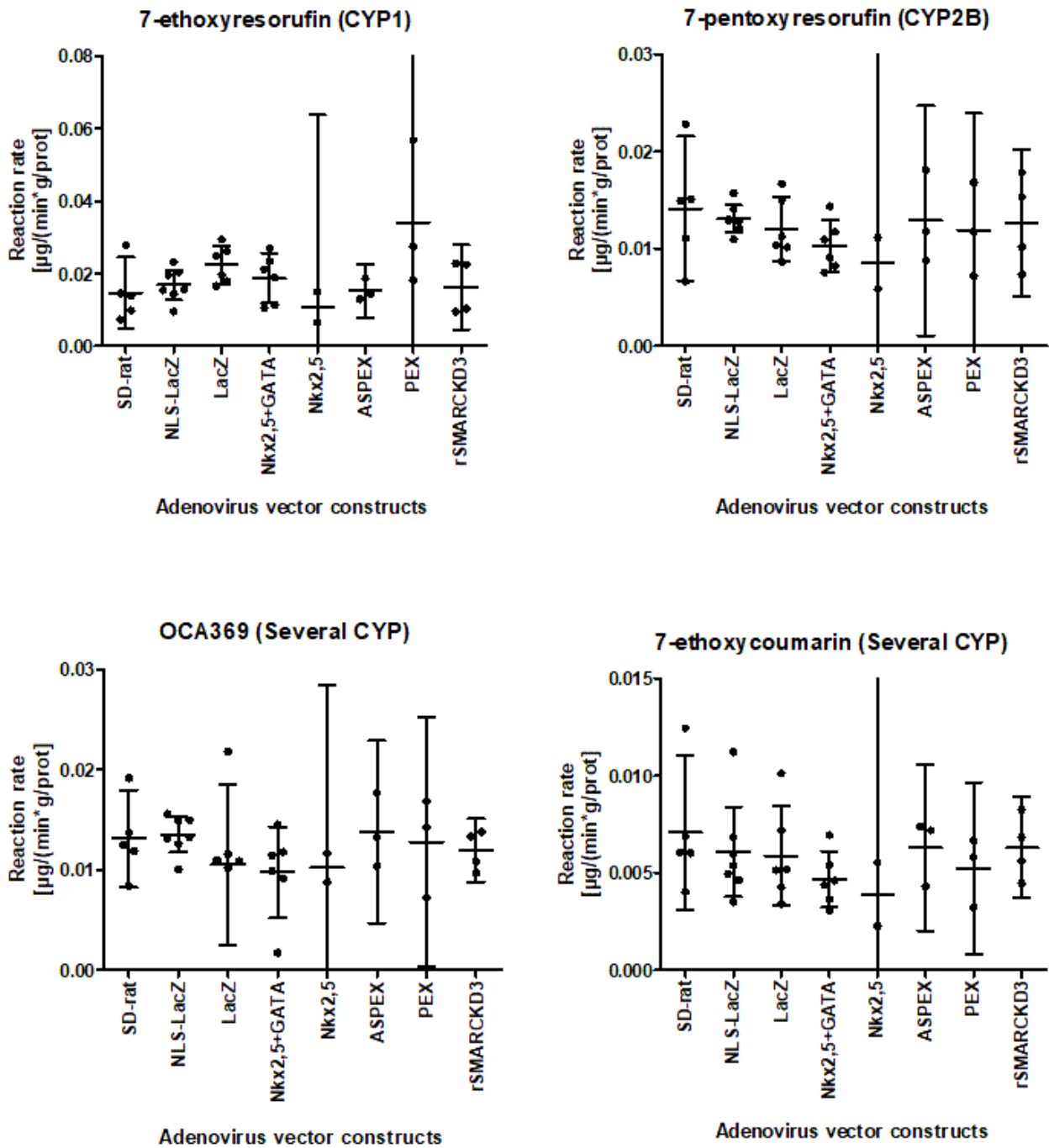


Figure 9. Liver CYP enzyme activities of rats treated with adenovirus vector constructs. 7-Ethoxyresorufin is probe substrate of CYP1, 7-pentoxoresorufin) of CYP2B, OCA369) and 7-ethoxycoumarin of several CYPs.

5.2 Conjugation reactions

Experiment 5 (HFC) measuring the glucuronidation pathway did not show significant differences between the groups (Figure 10). The largest difference between averages was observed in treatment group Nkx2.5 compared to the control (a decrease of 51%). However, the Nkx2.5 group has only two samples, therefore this is likely due to random error and the difference is not statistically significant ($p=0.0783$, $p>0.05$). HFC glucuronidation did show weak correlation with HFC sulfonation experiment 6 ($r=-0.271$) and esculetin methylation ($r=-0.315$), and no correlation with CDNP glutathione conjugation ($r=-0.045$).

Experiment 6 (HFC) measuring the sulfonation pathway does not show significant differences between the groups (Figure 10). The largest difference between reaction rate averages was observed in the treatment group LacZ compared to the control (a decrease of 23%). However, the Nkx2.5 group has only two samples, therefore this is likely due to random error and the difference is not statistically significant ($p=0.1399$, $p>0.05$). HFC sulfonation did show moderate correlation with O-methylation of esculetin ($r=0.420$), and moderate correlation with CDNP glutathione conjugation ($r=0.579$).

Experiment 7 (HFC) measuring the O-methylation pathway does not show significant differences between the groups (Figure 10). The largest difference between reaction rate averages was observed in treatment groups Nkx2.5 compared to control (an increase of 124%). However, the Nkx2.5 group has only two samples, therefore this is very likely due to random error and the difference is not statistically significant ($p=0.2472$, $p>0.05$). HFC O-methylation did not show correlation with CDNP glutathione conjugation ($r=-0.033$).

Experiment 8 (CDNB) measuring the glutathione S-transferase pathway does not show significant differences between the groups (Figure 10). The largest difference between reaction rate averages is observed in treatment groups PEX and ASPEX compared to SD-rat (both decreased 41%). However, this is likely due to random error and the difference is not statistically significant ($p=0.3417$, $p>0.05$).

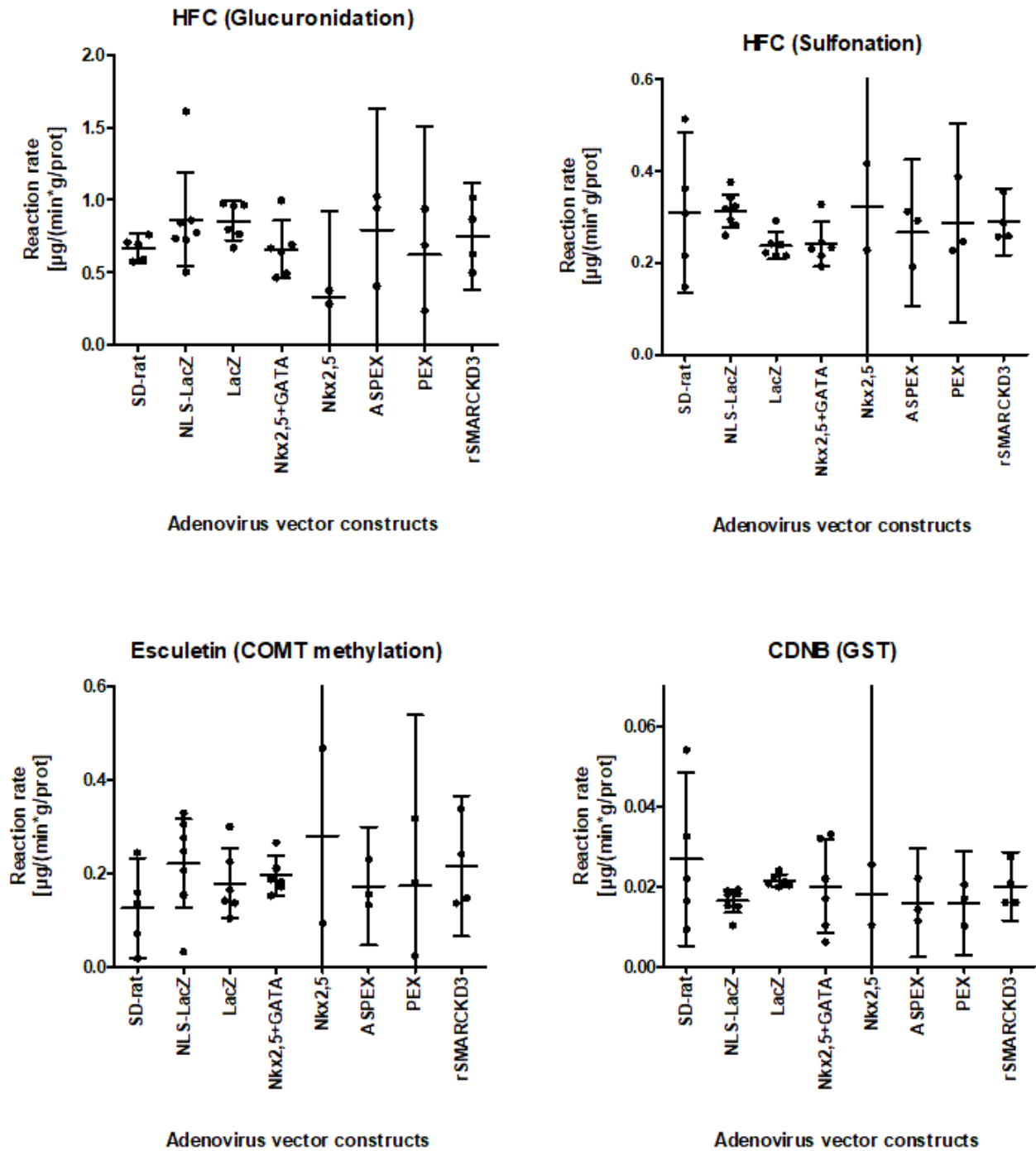


Figure 10. Liver conjugation enzyme activities of rats treated with adenovirus vector constructs. HFC was used to measure glucuronidation activity and sulfonation activity. Esculetin was the probe substrate for COMT and CDNB was the probe substrate for GST.

The principal component analysis does not show a clear separation of the active treatment group when compared to the no treatment or mock treatment groups (Figure 11). The first principal component (x-axis) explains 32%, and the second component (y-axis) explains 24%, of the variance in the data.

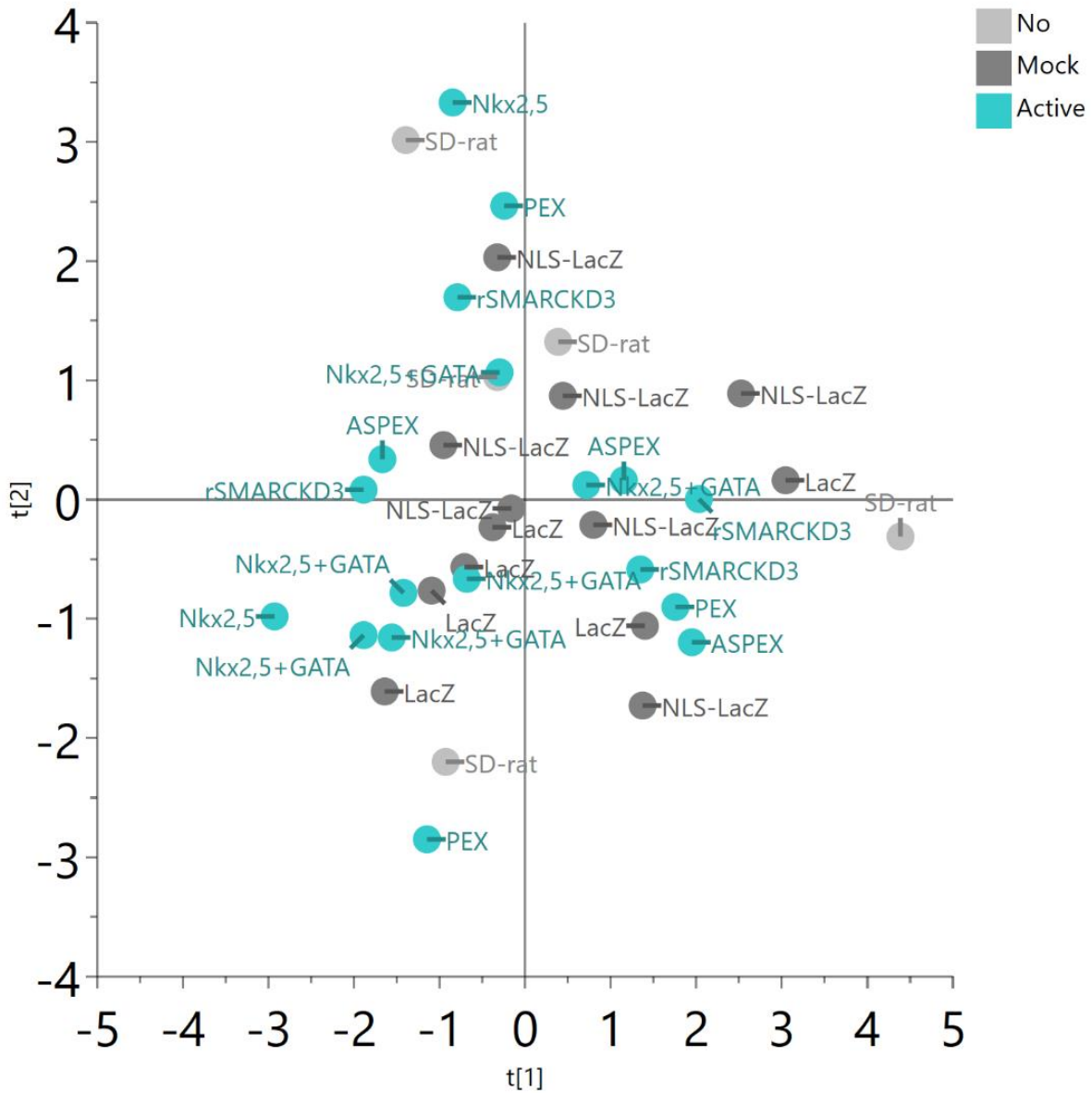


Figure 11. Results from the multivariate analysis.

6 Discussion

This study aimed to find out if recombinant adenovirus transgenes cause alteration in xenobiotic metabolic enzyme activities in rat liver. Adenoviral gene transfer did not cause significant changes in liver xenobiotic-metabolizing enzyme activity after 14 days of the treatment. The expectation for the results of this study was that all viruses studied should decrease metabolic activity unless the transgene they are carrying is somehow able to counteract this effect. The results of the study were not consistent with the hypothesis that enzyme activity would decrease. Previous studies have found that AdVs are targeted in the liver in mice, AdV without a transgene can cause a decrease in xenobiotic metabolism enzyme activities, and in general, viral infections decrease xenobiotic metabolism enzyme activities (Shayakhmetov et al. 2005, Callahan et al. 2008, Klaasen 2019).

The largest decrease in the whole study was observed in glucuronidation activity with Nkx2.5 treatment, which had 51% lower enzyme activity compared to control (experiment 5). However, this could be due to random error, since Nkx2.5 had only two samples (p -value = 0.0783). Results of experiment 2 (7-pentoxoresorufin) and experiment 4 (7-ethoxycoumarin) look similar and they had significant correlation among each other ($r=0.781$), therefore they measure the same thing. This could mean that the CYP2B enzymes are regulated similarly compared to CYP other enzymes in rats. Another explanation could be that 7-ethoxycoumarin and 7-pentoxoresorufin were metabolised mainly by the same CYP2 enzymes. The largest increase in the whole study was observed in CYP1 activity with PEX treatment, which had 132% higher reaction rate compared to control (experiment 1). This was not statistically significant either due to low sample numbers and high variation. COMT methylation activity slightly higher in all viral treatments with an average change of 64 percentage points ($\sigma = 31$ percentage points, experiment 7). GST activity slightly lower in all viral treatments with an average change of -32 percentage points ($\sigma = 9$ percentage points, experiment 8). 95% confidence interval overlap almost in all groups, and no statistically significant changes were observed. Therefore, the results of the experiments suggest that AdV or functional transgenes used in this study did not cause significant changes in xenobiotic-metabolizing enzyme

activities after 14 days of the treatment. Baseline CYP enzyme concentrations between individuals can range from 2-36 -fold, therefore changes of less than -50% to 100% have minimal biological significance (Snawder and Lipscomb 2000). Therefore, likely there is no need for long term dose adjustments of other drugs in the context of adenoviral treatment with transgenes used in this study.

In this study, rats were killed 14 days after the administration of AdV. Protein expression caused by adenoviral vectors is short-lived (weeks) (Bouard et al. 2009). Therefore, possible alterations in the metabolic activity were already mostly restored. A reduction of 70% after 24-hours and 56% after 48-hours was observed in hepatic CYP3A catalytic activity when mice were infected with AdlacZ recombinant adenovirus of serotype 5 (Jonsson-Schmunk et al. 2016). This suggests that activity changes may occur before the time point of 14 days. Unlike the previous study, the methods used in this paper measure if substrates are metabolized, but mRNA levels or the amount of the specific enzyme responsible for catalysing the reactions were not determined.

There are some limitations in the study. These results do not qualify for reliable safety information as there are some issues with statistical power due to low sample numbers. To improve this study, there should be more samples. The degree of freedom in this study was 4 in the worst case of Nkx2.5. To have at least a value of 10, there should be at least 6 samples in each group. This increase in sample numbers would eliminate the issues with wide 95% confidence intervals and give more statistical power. In addition to a sampling time point of 14 days, there should also be a time point of 7 days to see if AdV cause changes closer to the time point of administration. Plausible sources of error in this study were pipetting accuracy. Looking through reaction rates of parallel sample wells, a difference of 10-40% was common and a handful of the cases had more than 100% difference.

7 Conclusion

This study aimed to find out if recombinant adenovirus transgenes cause alteration in xenobiotic metabolic enzyme activities in rat liver. Differences in measured enzyme activities between treatments and controls were not statistically significant. Additionally, individual variance in baseline enzyme expression can be more than 2-36-fold, in other words, less than -50% to 100% changes in enzyme activity are relatively small. Therefore, adenovirus vector or transgenes in this study did not cause significant changes in xenobiotic-metabolizing activity after 14 days of the treatment. A decrease in enzyme activity was expected based on information gained from previous studies, however, this was not seen in the results. In the light of these findings, likely there is no need for long term dose adjustments of other drugs in the context of adenoviral treatment with transgenes used in this study.

References

- Alaspää A: Terveysportti, Lääkärin käsikirja, Lääkemyrkytykset. Accessed 16.9.2021.
<https://www.terveysportti.fi/apps/dtk/ltk/article/ykt00408>
- Bergelson JM, Cunningham JA, Droguett G et al.: Isolation of a common receptor for coxsackie B viruses and adenoviruses 2 and 5. *Science* 275(5304): 1320-1323, 1997
- Bewley MC, Springer K, Zhang Y- et al.: Structural analysis of the mechanism of adenovirus binding to its human cellular receptor, CAR. *Science* 286(5444): 1579-1583, 1999
- Born S, Hu J, Lehman-Mckeeman L: O-hydroxyphenylacetaldehyde is a hepatotoxic metabolite of coumarin. *Drug Metab Disposition* 28(2): 218-223, 2000
- Bouard D, Alazard-Dany N, Cosset F: Viral vectors: From virology to transgene expression. *Br J Pharmacol* 157(2): 153-165, 2009
- Buckley R: Gene therapy for SCID—a complication after remarkable progress. *Lancet* 360(9341): 1185-1186, 2002
- Burckhardt CJ, Suomalainen M, Schoenenberger P et al.: Drifting motions of the adenovirus receptor CAR and immobile integrins initiate virus uncoating and membrane lytic protein exposure. *Cell host & microbe; Cell Host Microbe* 10(2): 105-117, 2011
- Callahan SM, Wonganan P, Croyle MA: Molecular and macromolecular alterations of recombinant adenoviral vectors do not resolve changes in hepatic drug metabolism during infection. *Virology journal; Virol J* 5(1): 111, 2008
- EMA: Jcovden (previously COVID-19 Vaccine Janssen). Accessed May 18,2022.
<https://www.ema.europa.eu/en/medicines/human/EPAR/jcovden-previously-covid-19-vaccine-janssen>
- EMA: Vaxzevria (previously COVID-19 Vaccine AstraZeneca). Accessed May 18,2022.
<https://www.ema.europa.eu/en/medicines/human/EPAR/vaxzevria-previously-covid-19-vaccine-astrazeneca>
- Feng L, Ning J, Tian X et al.: Fluorescent probes for the detection and imaging of cytochrome P450. *COORDIN CHEM REV* 437: 213740, 2021
- Finnish institute for health and welfare: Adenovirus vaccines: FAQ. Accessed May 18,2022.
<https://thl.fi/en/web/infectious-diseases-and-vaccinations/what-s-new/coronavirus-covid-19-latest-updates/vaccines-and-coronavirus/adenovirus-vaccines-faq>
- Fisher MB, Paine MF, Strelevitz TJ et al.: The role of hepatic and extrahepatic UDP-glucuronosyltransferases in human drug metabolism. *Drug Metab Rev* 33(3-4): 273-297, 2001

- Gallardo J, Pérez-Illana M, Martín-González N et al.: Adenovirus structure: What is new?. *International journal of molecular sciences* 22(10): 5240, 2021
- Giacca M, Zacchigna S: Virus-mediated gene delivery for human gene therapy. *J Controlled Release* 161(2): 377-388, 2012
- Goodman LS, Brunton LL, Chabner BA, Knollmann BC: Goodman & Gilman's the pharmacological basis of therapeutics. 12. ed. McGraw-Hill, New York 2011
- Greber UF, Suomalainen M, Stidwill RP et al.: The role of the nuclear pore complex in adenovirus DNA entry. *EMBO J* 16(19): 5998-6007, 1997
- Huang W, Lin YS, McConn DJ et al.: Evidence of significant contribution from CYP3A5 to hepatic drug metabolism
. *Drug Metab Disposition* 32(12): 1434-1445, 2004
- IUBMB: Recommendations of the Nomenclature Committee of the International Union of Biochemistry and Molecular Biology on the Nomenclature and Classification of Enzymes by the Reactions they Catalyse. Accessed 25 May, 2022. <https://iubmb.qmul.ac.uk/enzyme/>
- Jonsson-Schmunk K, Wonganan P, Choi JH et al.: Integrin receptors play a key role in the regulation of hepatic CYP3A. *Drug Metab Disposition* 44(5): 758-770, 2016
- Juan CA, de la Lastra, José Manuel Pérez, Plou FJ et al.: The chemistry of reactive oxygen species (ros) revisited: Outlining their role in biological macromolecules (dna, lipids and proteins) and induced pathologies. *INT J MOL SCI* 22(9): 4642, 2021
- Juvonen RO, Ahinko M, Huuskonen J et al.: Development of new coumarin-based profluorescent substrates for human cytochrome P450 enzymes. *Xenobiotica* 49(9): 1015-1024, 2019
- Klaasen CD: Casarett and Doull's toxicology : The basic science of poisons. 9. ed. McGraw-Hill Education LLC, New York, N.Y 2019
- Lake B: Coumarin metabolism, toxicity and carcinogenicity: Relevance for human risk assessment. *Food Chem Toxicol* 37(4): 423-453, 1999
- Lasaro MO, Ertl HCJ: New insights on adenovirus as vaccine vectors. *Mol Ther* 17(8): 1333-1339, 2009
- Lee C, Bishop E, Zhang R et al.: Adenovirus-mediated gene delivery: Potential applications for gene and cell-based therapies in the new era of personalized medicine. *Genes & Diseases; Genes Dis* 4(2): 43-63, 2017
- Lee D, Liu J, Junn HJ et al.: No more helper adenovirus: Production of gutless adenovirus (GLAd) free of adenovirus and replication-competent adenovirus (RCA) contaminants. *Exp Mol Med* 51(10): 1-18, 2019

- Lenman A, Liaci AM, Liu Y et al.: Polysialic acid is a cellular receptor for human adenovirus 52. *Proc Natl Acad Sci U S A* 115(18): E4264-E4273, 2018
- Lewis D, Ito Y, Lake B: Metabolism of coumarin by human P450s: A molecular modelling study. *Toxicol In Vitro* 20(2): 256-264, 2006
- Lin JH: Species similarities and differences in pharmacokinetics. *Drug Metab Dispos* 23(10): 1008-1021, 1995
- Long R, Rickert D: Metabolism and excretion of 2,6-dinitro [14C] toluene in vivo and in isolated perfused rat livers. *Drug Metab Disposition* 10(5): 455-458, 1982
- Lundstrom K: Viral vectors for COVID-19 vaccine development. *Viruses; Viruses* 13(2): 317, 2021
- Marttila M, Persson D, Gustafsson D et al.: CD46 is a cellular receptor for all species B adenoviruses except types 3 and 7. *J Virol* 79(22): 14429-14436, 2005
- Meier O, Greber UF: Adenovirus endocytosis. *J Gene Med* 5(6): 451-462, 2003
- Morgan ET, Goralski KB, Piquette-Miller M et al.: Regulation of drug-metabolizing enzymes and transporters in infection, inflammation, and cancer. *Drug Metab Disposition* 36(2): 205-216, 2008
- Murphy RC, Zarini S: Glutathione adducts of oxyeicosanoids. *Prostaglandins Other Lipid Mediat* 68: 471-482, 2002
- National Institutes of Health, Health & Human Services, Freedom of Information Act: MeSH Descriptor Data 2021, Xenobiotics
. Accessed 3.8.2021. <https://meshb.nlm.nih.gov/record/ui?ui=D015262>
- Nemerow GR, Stewart PL: Insights into adenovirus uncoating from interactions with integrins and mediators of host immunity. *Viruses; Viruses* 8(12): 337, 2016
- Ortega-Esteban A, Pérez-Berná AJ, Menéndez-Conejero R et al.: Monitoring dynamics of human adenovirus disassembly induced by mechanical fatigue. *Scientific reports; Sci Rep* 3(1): 1434, 2013
- Ortega-Esteban A, Condezo GN, Pérez-Berná AJ, et al.: Mechanics of viral chromatin reveals the pressurization of human adenovirus. *ACS nano; ACS Nano* 9(11): 10826-10833, 2015
- Parks RJ, Chen L, Anton M et al.: A helper-dependent adenovirus vector system: Removal of helper virus by cre-mediated excision of the viral packaging signal. *Proc Natl Acad Sci U S A* 93(24): 13565-13570, 1996
- Pérez-Berná A.J., Ortega-Esteban A, Menéndez-Conejero R et al.: The role of capsid maturation on adenovirus priming for sequential uncoating. *J Biol Chem* 287(37): 31582-31595, 2012

- Pérez-Berná A.J., Marabini R, Scheres SHW et al.: Structure and uncoating of immature adenovirus. *J Mol Biol* 392(2): 547-557, 2009
- Ranta V, Honkakoski P, Vellonen K, Ruponen M: *Farmakokinetiikan perusteet*. 1. ed. Farmasian opiskelijayhdistys Fortis ry, Kuopio 2017
- Raper S, Chirmule N, Lee F et al.: Fatal systemic inflammatory response syndrome in a ornithine transcarbamylase deficient patient following adenoviral gene transfer. *Mol Genet Metab* 80(1): 148-158, 2003
- Rath VL, Verdugo D, Hemmerich S: Sulfotransferase structural biology and inhibitor discovery. *Drug Discov Today* 9(23): 1003-1011, 2004
- Raunio H, Pentikäinen O, Juvonen RO: Coumarin-based profluorescent and fluorescent substrates for determining xenobiotic-metabolizing enzyme activities in vitro. *INT J MOL SCI* 21(13): 1-17, 2020
- Rux J, Burnett R: Adenovirus structure. *Hum Gene Ther* 15(12): 1167-1176, 2004
- Shayakhmetov DM, Gaggar A, Ni S et al.: Adenovirus binding to blood factors results in liver cell infection and hepatotoxicity. *J Virol* 79(12): 7478-7491, 2005
- Sim E, Abuhammad A, Ryan A: Arylamine n-acetyltransferases: From drug metabolism and pharmacogenetics to drug discovery. *Br J Pharmacol* 171(11): 2705-2725, 2014
- Snawder JE, Lipscomb JC: Interindividual variance of cytochrome P450 forms in human hepatic microsomes: Correlation of individual forms with xenobiotic metabolism and implications in risk assessment. *Regul Toxicol Pharmacol* 32(2): 200-209, 2000
- Stasiak AC, Stehle T: Human adenovirus binding to host cell receptors: A structural view. *Med Microbiol Immunol (Berl)* 209(3): 325-333, 2020
- Tenhunen O, Rysä J, Ilves M et al.: Identification of cell cycle regulatory and inflammatory genes as predominant targets of p38 mitogen-activated protein kinase in the heart. *Circ Res* 99(5): 485-493, 2006
- Terveysportti: Terveysportti, lääketietokanta. Accessed 16.9.2021.
<https://www.terveysportti.fi/apps/laake/>
- Tilemann L, Ishikawa K, Weber T et al.: Gene therapy for heart failure. *Circ Res* 110(5): 777-793, 2012
- Tukey RH, Strassburg CP: Human UDP-glucuronosyltransferases: Metabolism, expression, and disease. *Annu Rev Pharmacol Toxicol* 40(1): 581-616, 2000
- Tukey R, Strassburg C: Human UDP-glucuronosyltransferases: Metabolism, expression, and disease. *Annu Rev Pharmacol* 40(1): 581-616, 2000

Wang H, Liu Y, Koyuncu D et al.: Desmoglein 2 is a receptor for adenovirus serotypes 3, 7, 11 and 14. *Nat Med* 17(1): 96-104, 2011

Wiethoff CM, Wodrich H, Gerace L et al.: Adenovirus protein VI mediates membrane disruption following capsid disassembly. *J Virol* 79(4): 1992-2000, 2005

Willison HJ, Bauer J, Johansson SMC et al.: The GD1a glycan is a cellular receptor for adenoviruses causing epidemic keratoconjunctivitis. *Nat Med* 17(1): 105-109, 2011

Ylä-Herttuala S, Baker AH: Cardiovascular gene therapy: Past, present, and future. *Mol Ther* 25(5): 1095-1106, 2017

Appendices

Appendix 1. Example of enzyme assay protocol, experiment 7 had different setup for standard wells using mixture of esculetin and scopoletin.

Experiment 7. Esculetin O-methylation activity of different cytosols of rats livers.

Background: Esculetin is the methylated substrate for catechol O-methyltransferase (COMT).

Aim of this experiment is to determine COMT activity in liver cytosols of rats and to see if adenovirus treatment affects the level of HFC sulfonation.

Reagents of one experiment

1 M, 100 mM and 10 mM phosphate pH 7.4

0.1 M MgCl₂

100 mM MgCl₂

1 mM S-adenosylmethionine in 10 mM phosphate pH 7.4.

10 mM esculetin. Do 1 mM esculetin 10 µL 10 mM esculetin +90 µL DMSO.

Liver cytosols

Standard stock of 1 mM Scopoletin. Scopoletin and esculetin mixture standards in 100 mM Phosphate pH 7.4

Dilute them to

10 µM Esculetin: 5 µL 1mM Esculetin + 495 µL 100 mM Phosphate pH 7.43 µL

9 µM Es 1 µM Sc (4.5 µL 1 mM Es + 0.5 µL 1 mM Sc + 495 µL 100 mM Phosphate pH 7.4),

8 µM Es 2 µM Sc (4 µL 1 mM Es + 1 µL 1 mM Sc + 495 µL 100 mM Phosphate pH 7.4),

7 µM Es 3 µM Sc (3.5 µL 1 mM Es + 1.5 µL 1 mM Sc + 495 µL 100 mM Phosphate pH 7.4),

6 µM Es 4 µM Sc (3 µL 1 mM Es + 2 µL 1 mM Sc + 495 µL 100 mM Phosphate pH 7.4),

5 µM Es 5 µM Sc (2.5 µL 1 mM Es + 2.5 µL 1 mM Sc + 495 µL 100 mM Phosphate pH 7.4),

4 µM Es 6 µM Sc (2 µL 1 mM Es + 3 µL 1 mM Sc + 495 µL 100 mM Phosphate pH 7.4),

3 µM Es 7 µM Sc (1.5 µL 1 mM Es + 3.5 µL 1 mM Sc + 495 µL 100 mM Phosphate pH 7.4),

2 µM Es 8 µM Sc (1 µL 1 mM Es + 4 µL 1 mM Sc + 495 µL 100 mM Phosphate pH 7.4),

1 µM Es 9 µM Sc (0.5 µL 1 mM Es + 4.5 µL 1 mM Sc + 495 µL 100 mM Phosphate pH 7.4),

10 µM Sc (5 µL 1 mM Sc + 495 µL 100 mM Phosphate pH 7.4),

0 µM (500 µL 100 mM Phosphate pH 7.4)

Experiment

O-methylation with cytosol

Reagents	R1	B1	Incubation concentration
1 M Phosphate pH 7.4	10 µL	10 µL	100 mM
100 mM MgCl ₂	5 µL	5 µL	
Liver cytosol	1 µL	--	
H ₂ O	73.9 µL	73.9 µL + 1 µL	

1 mM S-adenosylmethionine 10 μ L 10 μ L

10 mM Esculetin 0.1 μ L 0.1 μ L

Pipet 100 μ L standards of Es and Sc to the wells H 1-12

Pre-warm the Victor to 37°C.

Make pool (100 X) 1000 μ L 1 M Phosphate pH 7.4, 7390 μ L water, 10 μ L 10 mM Esculetin and 500 μ L 100 mM MgCl₂. Mix.

Pipet 1 μ L cytosol to wells A-G 1-12 and 1 μ L water to blank samples G 9-12.

Pipet 89 μ L pool for cytosols to the wells A-G 1-12.

Pre-incubate the plate and S-adenosylmethionine for 5 min at 37°C.

Pipet 10 μ L 1 mM S-adenosylmethionine to all A-G 1-12 wells. DO NOT PIPET IT TO H 1-12.

Start the Risto Coumarin derivatives kinetic protocol in Victor.

	1	2	3	4	5	6	7	8	9	10	11	12
A	1	1	2	2	3	3	4	4	5	5	6	6
B	7	7	8	8	9	9	10	10	11	11	12	12
C	13	13	14	14	15	15	16	16	17	17	18	18
D	19	19	20	20	21	21	22	22	23	23	24	24
E	25	25	26	26	27	27	28	28	29	29	30	30
F	31	31	32	32	33	33	34	34	35	35	36	36
G	37	37	38	38	39	39	40	40	Bl	Bl	Bl	Bl
H	St 0	E10S0	E9S1	E8S2	E7S3	E6S4	E5S5	E4S6	E3S7	E2S8	E1S9	E0S10

Appendix 2. Experiment 8 protocol

Experiment 8. Glutathione S-transferase activity of different cytosols of rats livers.

Background: Glutathione is the most important nucleophilic defense against electrophilic xenobiotics and metabolites formed in drug metabolism. Glutathione S-transferase enzymes catalyze the conjugation of electrophilic substances to glutathione conjugates. Most of them are cytosolic enzymes. 1-Chloro-2,4-dinitrobenze (CDNB) is multienzyme substrate for GSTs.

This experiment aims to determine GST activity in liver cytosols of rats and to see if adenovirus treatment affects this activity.

Reagents/Materials

0.1 M K-phosphate buffer pH 6.5

50 mM 1-chloro-2,4 dinitrobenzene (CDNB) in DMSO. MW is 202,55 g/mol

10 mM GSH

Cytosol samples of rat livers

Distilled water

Protect CDNB from light with aluminum paper and prepare 50 mM before use w/ 10.1 mg/1ml DMSO

Prepare 10 mM GSH (MW 307 g/mol) in K-phosphate buffer (3.1 mg/ 1 ml) before use. Prepare it daily

Method

Reagents	Reaction	No reaction		
100 mM phosphate pH 7.4	171 μ L	171 μ L		
Cytosol	5	--		
50 mM CDNB	4 μ L	4 μ L		
H2O	0 μ L	5 μ L		
10 mM GSH	20 μ L	20 μ L		

Pre-warm the Hidex to 37°C.

Make pool (100 X) 17 100 µL 100 mM Phosphate pH 7.4, 400 µL 50 mM CDNB. Mix.

Dilute liver cytosols 1:20: 5 µL cytosol and 95 µl 100 mM phosphate pH 7.4.

Pipet 5 µL cytosol to wells A-G 1-12 and 5 µL water to blank samples G 9-12. Use transparent multi-well plate, because absorbance is measured.

Pipet 175 µL pool for cytosols and blanks to the wells A-G 1-12.

Pre-incubate the plate and glutathione for 5 min at 37°C.

Pipet 20 µl 10 mM glutathione to all A-G 1-12 wells. DO NOT PIPET IT TO H 1-12.

Start the GST protocol of absorbance technology in Hidex.

Appendix 3. Reaction rate averages as a table

Table 5. Average reaction rates of rats treated with different viral gene cassettes. Colours compared to untreated SD-rat reaction rates, where red is lower reaction rate and blue is higher reaction rate.

Average reaction rates in each virus group ($\mu\text{g}/(\text{min} \cdot \text{g}/\text{prot})$)										
Virus	EXP1	EXP2	EXP3	EXP4	EXP5	EXP6	EXP7	EXP8	Group average	Group avg / SD avg
SD-rat	0,0147	0,0141	0,0131	0,0071	0,6644	0,3088	0,1251	0,0268	0,1468	0,000
LacZ	0,0225	0,0120	0,0105	0,0059	0,8549	0,2374	0,1778	0,0214		0,143
Nkx2.5+GATA	0,0187	0,0103	0,0098	0,0047	0,6585	0,2400	0,1946	0,0201		
Nkx2.5	0,0108	0,0085	0,0102	0,0039	0,3287	0,3218	0,2798	0,0179	0,1227	-0,164
ASPEX				0,0063	0,7912	0,2652	0,1721	0,0159		0,101
PEX	0,0341	0,0119	0,0128	0,0052	0,6198	0,2868	0,1731	0,0159		-0,012
rSMARCKD3		0,0127	0,0119	0,0063	0,7510	0,2895	0,2149	0,0200		0,126
NLS-LacZ				0,0061	0,8643	0,3129	0,2210	0,0164	0,1830	0,247
Virus avg	0,0189	0,0116	0,0118	0,0055	0,6955	0,2791	0,2048	0,0182		0,0606
Virus avg / SD-rat	0,2874	-0,1770	-0,1022	-0,2271	0,0468	-0,0964	0,6372	-0,3204		